The Dynamic Performance and Economic Benefit of a Blended Braking System in a Multi-Speed Battery Electric Vehicle

Jiageng Ruan[1*], Paul D. Walker[1], Peter A. Watterson[1], Nong Zhang[1]

1 University of Technology Sydney, 15 Broadway, Ultimo, NSW 2007, Australia

*Corresponding Author, Email Address: Jiageng.Ruan@student.uts.edu.au

Abstract

As motor-supplied braking torque is applied to the wheels in an entirely different way to hydraulic friction braking systems and it is usually only connected to one axle complicated effects such as wheel slip and locking, vehicle body bounce and braking distance variation will inevitability impact on the performance and safety of braking. The potential for braking energy recovery in typical driving cycles is presented to show its benefit in this study. A general predictive model is designed to analysis the economic and dynamic performance of blended braking systems, satisfying the relevant regulations/laws and critical limitations. Braking strategies for different purposes are proposed to achieve a balance between braking performance, driving comfort and energy recovery rate. Special measures are taken to avoid any effects of motor failure. All strategies are analyzed in detail for various braking events. Advanced driver assistance systems (ADAS), such as ABS and EBD, are properly integrated to work with the regenerative braking system (RBS) harmoniously. Different switching plans during braking are discussed. The braking energy recovery rates and brake force distribution details for different driving cycles are simulated. Results for two of the cycles in an 'Eco' mode are measured on a drive train test rig and found to agree with the simulated results to within approximately 10%. Reliable conclusions can thus be gained on the economic benefit and dynamic braking performance. The strategies proposed in this paper are shown to not only achieve comfortable and safe braking during all driving conditions, but also to significantly reduce cost in both the short and long term.

Keywords: Regenerative braking; Blended braking system; Strategy; Cost; Driving cycles.

1. Introduction

The benefit of regenerative braking by blended braking systems, combining electric and friction brakes, has been theoretically and experimentally validated in many kinds of electric vehicle (EV), e.g. battery electric vehicle (BEV) [1,2], fuel cell electric vehicle (FEV) [3], and hybrid electric vehicle (HEV) [4]. A plethora of similar papers can be found which focus on braking energy recovery improvement by optimizing strategies and studying the performance of braking system itself. Nian, at al used PID control and fuzzy logic in a brushless DC motor to realize regenerative braking and prolong driving range, ensuring the braking quality at the same time [5]. A vehicle lateral motion state based adaptive control strategy was proposed by Han and Park to guarantee the vehicle controllability and stability [6]. Electromechanical brake was

integrated into regenerative braking to ensure braking force distribution ratio follow an optimal curve, instead of a linear line [7]. According to the results from Gao, et al, blended braking system structure plays an important role in energy recovery rate [8]. Zhang developed a regenerative braking system by utilizing as much as possible mature components, integrating cooperative regeneration with Anti-lock Braking System (ABS)/Traction Control System (TCS) functions, which provided system reliability, low development cost and risk at the same time [9]. Battery current balance during regenerative braking was investigated in [10] by experimental analysis in both used-defined and FTP-75 driving cycles.

However, the frequently mentioned energy recovering ability and braking performance, in the above studies, are just two of the key factors in blended braking system design, and are not mutually independent. The safety issues introduced by the addition of a brake-by-wire system, the braking performance affected by a combination strategy, the potential economic benefits, and the relationship of economic benefit and braking performance need to be considered as well. Specially testing maneuvers for blended braking system, which are often neglected by many studies, are required to validate the braking performance in all conditions [11,12]. The problems became more complicated when a multi-speed gearbox became popular on EVs, such as an Automatic Transmission (AT), Automated Manual Transmission (AMT) or Continuously Variable Transmission (CVT) is added to improve the dynamic performance and driving range, then additional problems of response delay and torque interruption are introduced [13–15]. These problems are of particular concern for the simplified two-speed Dual Clutch Transmission (DCT), which has been proven to be extremely suitable for EVs [16,17]. Additionally, safety-oriented driver assistance system, such as the Anti-lock Braking System (ABS) and Electronic Brake Force Distribution (EBD), should also be integrated into blended braking strategies properly to ensure their effectiveness [18,19]. At last, for any of these complicated powertrain architectures, specially designed braking algorithms are needed to ensure safe braking, while recapturing as much kinetic energy as possible.

In this paper, an optimized blended braking strategy with a manual/automatic switch over function is proposed to achieve the balance between braking performance and energy recovery ability. This demonstrates the energy recovering improvement based economic benefit. A comprehensive investigation of the energy recovery, safety issues, braking dynamic performance, and economic benefit of a multi-speed transmission based blended braking system is clearly addressed.

Based on the achievement and limitations of previous papers, a brief breakdown of the comprehensive researching work, regarding to the dynamic performance and economic benefit of braking energy recovering on multi-speed BEV, is presented in following parts:

1. The energy lost in conventional friction braking is reported to indicate the maximum potential gains from regenerative braking,
2. The strengths and weaknesses of blended braking in a two-speed DCT based front-drive BEV are discussed.

3. The advantage of load transfer to the motor-connected front axle during braking is examined, while the torque interruption in gear shifting presents a disadvantage.
4. Different strategies are designed to either recapture maximum braking energy, or achieve the best braking performance, or to compromise between energy recovery and braking performance.
5. A simulation model is established to analyse the details of braking force distribution, wheel slip, and kinetic energy recovery rates in various test conditions.
6. One of the strategies is validated experimentally on an electric powertrain test bench for city and highway driving cycles.
7. Finally, the economic benefit of blended braking systems with different strategies is evaluated, in terms of fuel cost, initial manufacturing cost and maintenance cost.
8. Superior dynamic performance and economic benefit are obtained than for the strategies used in another recent study [20].

Some of the above content has been presented in paper [21] by a subset of the authors. That content is included here for completeness, but the content is restructured and rewritten, and extended with the new results on the brake force distribution, dynamic performance and economic benefit analysis of energy recovering.

2. Maximum Kinetic Energy Recovery

In EVs, regenerative braking captures the drop in the vehicle's kinetic energy, which in traditional Internal Combustion Engine (ICE) vehicles is lost as heat in friction brakes. However, the different working principles and the potential safety risks have been barriers to large-scale commercialization. To assess whether it is worth the extra cost of additional equipment and R&D to achieve a blended braking system for EVs, one must know the potential gain, i.e. how much energy is consumed by braking.

Fig.1 shows the distributions of energy consumption in several typical driving cycles for a medium size passenger Battery Electric Vehicle (BEV), without regenerative braking. The results are based on the integral of driving energy consumption and energy lost in friction braking with respect to time. The dynamic energy consumption in driving of specification Table 1A, i.e. rolling, aerodynamic drag and acceleration, is calculated by Eq.1, which is the product of vehicle dynamic resistance and travel distance per computational step size. According to the target speed profile of cycles, the dynamic friction braking force is achieved in Simulink model, shown in Fig.2. For city or hybrid cycles, the energy wasted in braking is very high, e.g. 39% in the California Unified Cycle (LA92) and 35% in Urban Driving Dynamometer Schedules (UDDS). In fact, the energy wasted can easily go over 50% during peak commuting times in congested cities. Even in the highway cycle Highway Fuel Economy Testing (HWFET), with less acceleration and deceleration events, the braking loss is still a considerable 15%. Though not all of the energy can be recaptured, these figures show the significant potential for a regenerative braking system (RBS) to extend driving range, thus saving energy use cost.

$$\Delta E_{driving} = (\mathrm{mg}C_R \cos\varphi + \mathrm{mg}\sin\varphi + \mathrm{C_D A u^2}/21.15 + \delta \mathrm{m d_u}/\mathrm{d_t}) \times \Delta x \qquad (1)$$

where C_R is the rolling resistance coefficient, φ represents the slop degree, $\mathrm{C_D}$ is the aerodynamic drag coefficient, A is the front area, u is vehicle velocity in km/h, δm is the equivalent mass in acceleration including the rotational components. Δx represents the travel distance per computational step size in Simulink model.

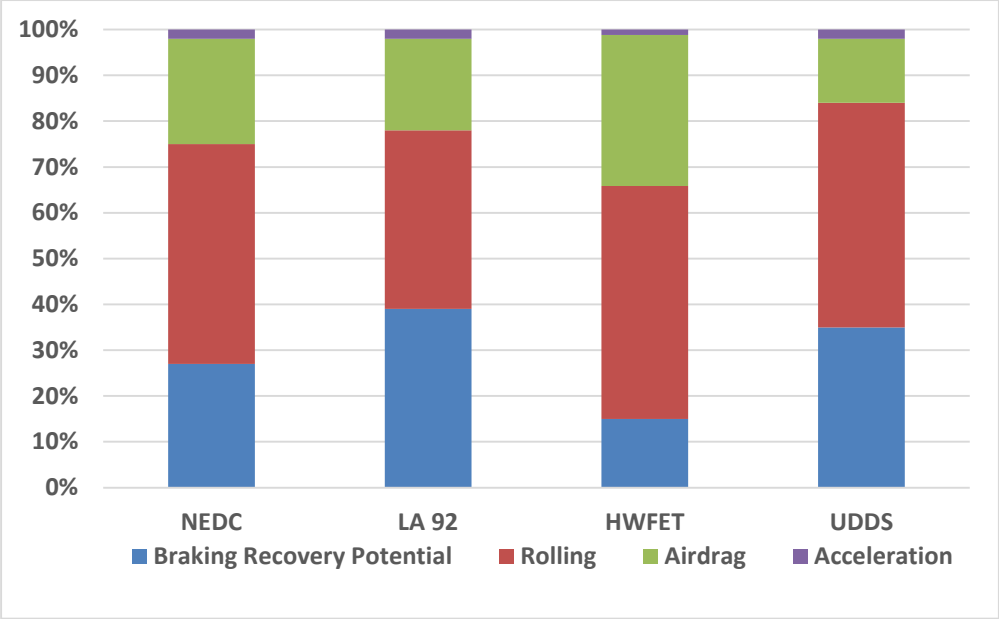

Figure 1: Energy consumption distribution in driving cycles, with the energy lost in braking shown in blue.

3. Powertrain Topology

The simulation model shown in Fig. 2 has been created to evaluate the safety and energy recovery performance of a blended braking system. It is a backward-facing model in which the desired driving cycle speed profile is assigned. For the given speed profile, the Vehicle Control Unit (VCU) calculates the required driving and braking torques and the power from the battery. The total required braking torque is apportioned in the 'Brake Torque Distribution' block into three command paths, to the front (axle) motor brake, the front friction brake, and the rear friction brake, according to the selected strategy. The regenerative braking torque is limited by the motor's maximum torque ability, which is a function of speed, and by the maximum charging current capability of the battery, which is a function of its state of charge. The motor torque goes through a stepped transmission, before being applied on the driven front axle. In the alternate torque command path, mechanical friction braking is directly applied to the wheels, front or rear, via a hydraulic system.

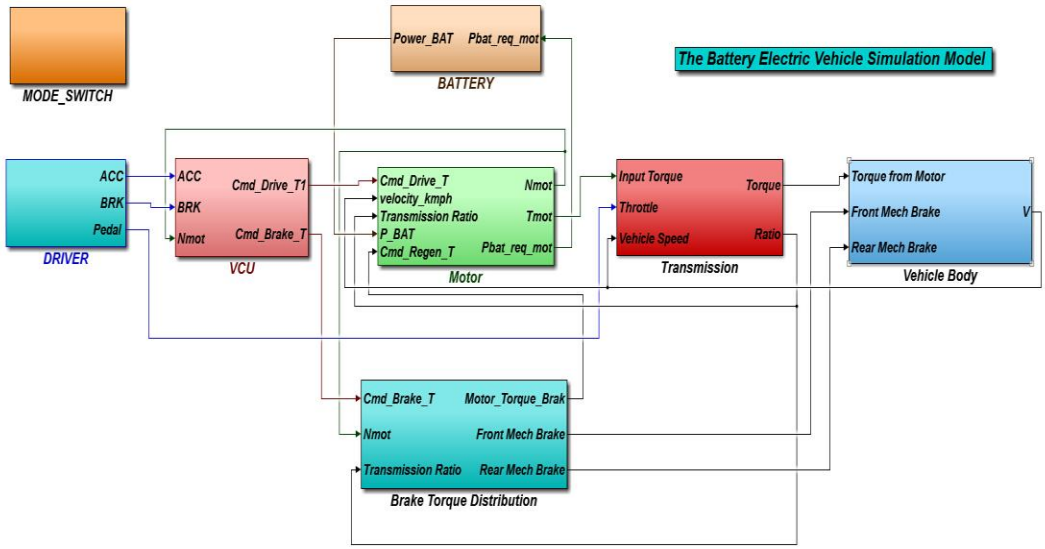

Figure 2: Two-speed DCT based BEV Simulink® model

The advantages and details of a two-speed DCT-based BEV have been introduced in Ref [22]. Here, only topics relating to braking in this new DCT structure are examined. Fig.3a depicts the two-speed DCT-based powertrain topology, and Fig.3b shows the powertrain's installation on the test bench used in this study. The test rig incorporates a high rotational inertia provided by four railway wheels to mimic the linear inertia of a moving vehicle.

The benefits of using front wheel drive in traditional ICE vehicles carry over to BEVs, such as lower cost, simpler design, control and manufacture, and greater boot space. Furthermore, for BEVs there is the additional advantage that regenerative braking has greater energy recovery potential on the front axle compared to the rear axle due to load transfer. The dynamic added weight on the front axle when braking or on the rear axle when accelerating is expressed:

$$\Delta Weight = amh_g/w \quad (2)$$

where a is the vehicle longitudinal acceleration, h_g is the height of the centre of mass, w is the wheelbase length and m is the total vehicle mass [23]. Fig.4 gives the ratio of the normal forces on the front and rear wheels at different deceleration rates of specification Table 1A. The ratio increases from 1.15 at constant speed to approximately 1.54 at 1 g (9.81 ms^{-2}) deceleration. The normal wheel load determines the maximum available friction force given the friction coefficient μ between a specific road and tyre, according to:

$$F_{friction} = \mu F_{normal} \quad (3)$$

a) b)

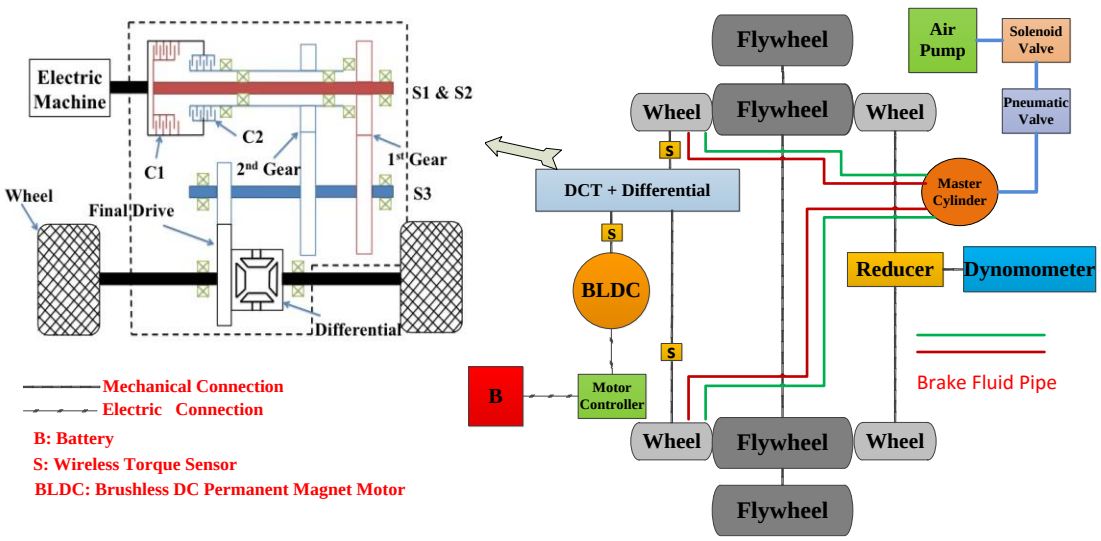

Figure 3: Schematic diagrams of: a) the Two-Speed DCT-based BEV powertrain topology; and b) the test bench.

Thus, the additional normal load on the front axle during braking enables greater regenerative braking from a front-mounted motor.

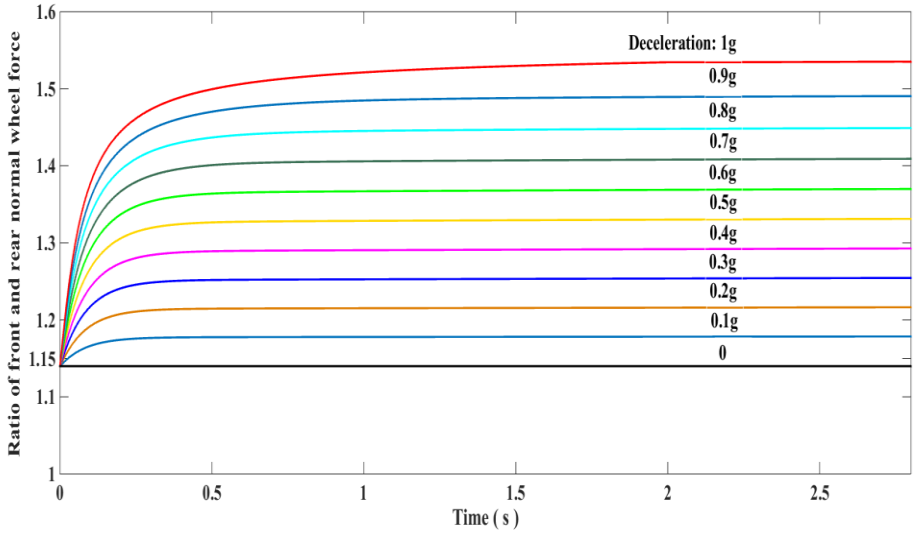

Figure 4: Ratio of the normal loads on the front and rear wheels during braking for a typical city vehicle chassis

4. Braking Regulations and Proposed Testing Maneuvers

In addition to the braking stability and performance testing procedures implemented in conventional vehicles, BEV which is equipped with a non-hydraulic RBS need specialized testing to isolate any potential system failures. For example, with the regenerated energy typically being deposited in the battery, any effect on the RBS from the battery being full charged must be tested.

In Europe, general safety requirements for new vehicles are legislated in Regulation (EC) No 661/2009 [24]. Specific requirements for braking systems are legislated by one or other of the following UNECE Regulations depending on the vehicle type and mass, the first Regulation applying to cars (category M1 being passenger vehicles of up to 8 passenger seats with maximum laden mass less than 3.5 tonnes):

- ECE Regulation 13H for light passenger vehicles (M1) and optionally light goods vehicles (N1) [25]
- ECE Regulation 13 for virtually all other vehicles [26]

ECE 13H and 13 divide the types of regenerative braking systems into three categories and describe the testing procedures in great detail [25],[27]:

- Category A: The electric regenerative system is not part of the ("service" or main) braking system. Typically, the function and the braking feeling reflected to the driver are similar to engine braking in ICE vehicles.
- Category B Non-Phased: The electric regenerative system is part of the braking system and regeneration commences or is increased when the brake is applied. The electric regenerative force starts to be developed at the same time as or slightly after the conventional friction brakes. This is also described as a parallel blended braking system.
- Category B Phased: The electric regenerative system is part of the braking system and the regenerative force can be developed ahead of any braking from the conventional friction brakes. This is also known as a serial blended braking system. This system allows the maximum amount of regenerative energy to be recovered.

Whichever the type of regenerative braking system, ECE 13H and 13 have the compulsory requirement of granting any Anti-Lock Braking System (ABS) an override priority to control braking. Similar procedures are presented in the United States National Highway Traffic Safety Administration [28].

To demonstrate compliance of the aforementioned regulations, the following specially designed maneuvers [27] and typical driving cycles are selected to test blended braking systems on BEV:

- Single straight line braking with piecewise braking force;
- The cooperation of ABS, Electronic Braking Force Distribution (EBD) and RBS;

- Load varying braking;
- Gear shift during braking;
- NEDC, UDDS, HWFET, LA92 and JP1015 [29–33];

5. Braking Strategies

5.1 Regenerative braking capability

Compared to hydraulic braking systems (HBS), the available regenerative braking torque is restricted by many factors, including the maximum available motor torque (which is a function of motor speed), the transmission gear ratios, and the maximum acceptable battery current. Therefore, the HBS must be ready to automatically compensate for any unexpected electric braking absence or diminishment, at any time. Furthermore, the HBS must be ready to adjust its braking output torque to an appropriate level to meet the driver's deceleration demand when the driving conditions change, for example if the vehicle hits a patch of ice.

The available regenerative braking on the front wheels is restricted by the motor peak output torque, the speed and the gear ratio. As we can see from Eq.5, the maximum braking force from the motor of specification Table 1A is limited to approximately 5 kN when the vehicle runs in 2nd gear. Even when the vehicle runs in 1st gear with a bigger torque amplification ratio, shown in Eq.4, the available maximum motor braking force is only 8 kN. Because the peak motor torque can only be supplied up to a certain speed, namely 2500 rpm for the motor of the specification of Table 1A, These maximum torques are only available during the starting period until each gear's 'turning point', given by Eq.6 and Eq.7, above which the maximum available braking torque drops as shown by the top operating boundary curves of Fig.5. For this reason, mechanical braking is still necessary for BEVs, in addition to the safety concerns.

For mild or moderate braking in the normal speed range, the required braking force can be supplied by the motor alone. However, under heavy braking or for the vehicle cruising at high speed, the motor has to cooperate with mechanical friction braking to stop the vehicle jointly.

$$Brake_{\max\_1}: T_{max} i_1 / r = 300 \times 8.45 / 0.3125 \; N = 8112 \; N \quad (4)$$

$$Brake_{\max\_2}: T_{max} i_2 / r = 300 \times 5.36 / 0.3125 \; N = 5146 \; N \quad (5)$$

$$Turning\ point\ vehicle\ speed\ in\ 1^{st}\ gear: \frac{2500 \times 2 \times pi \times 0.3125 \times 3.6}{8.45 \times 60} = 35 \; km \quad (6)$$

$$Turning\ point\ vehicle\ speed\ in\ 2^{nd}\ gear: \frac{2500 \times 2 \times pi \times 0.3125 \times 3.6}{5.36 \times 60} = 55 \; km \quad (7)$$

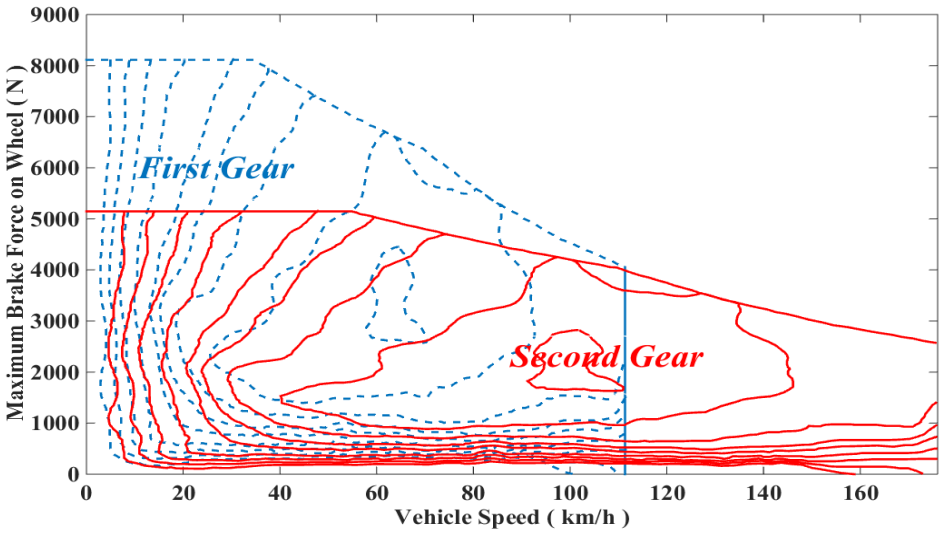

Figure 5: Available operating region of the motor braking force on the front wheels in different gears, also showing contours of motor efficiency.

5.2 Stability and controllability in braking

Backward-sloping colored lines in Fig.6 are the lines of constant total braking force, corresponding to the indicated deceleration values (as multiples of g). Eq.8 and Eq.9 give the maximum available friction force for front and rear tyres as a function of the road-tire friction coefficient.

$$F_{bf} = \mu mg\left(L_b + zh_g\right)/\mathrm{L} \quad (8)$$

$$F_{br} = \mu mg\left(L_a - zh_g\right)/L \quad (9)$$

where F_{bf} and F_{br} are the dynamic maximum friction force on front and rear wheels during decelerating based on load transfer. L_a and L_b are the distance from wheel centre to the CoM. The total maximum friction force is

$$Maximum\ (F_{bf} + F_{br}) = \mu mg \quad (10)$$

The vertical and horizontal black dash-dot lines represent the maximum available friction force based on different friction factors μ and the vehicle specification in Table.1A (see the Appendix). In other words, if the braking force applied to the wheels exceeds the critical threshold on a particular μ road, the wheel will lock. Generally, μ is less than 1.2, which means the maximum deceleration should be lower than 1.2g to avoid wheel locking, although the deceleration can go over 3g by improving vehicle aerodynamics structure and driving on a specially designed road, e.g. as is the case in Formula 1 racing. In this paper, considering the various road conditions and tire types used by the majority of passenger vehicles, which together determine

the friction factor, the maximum μ is set to 0.9 for safety at the cost of wasting some braking capability. The two red dash-dot bolt lines in Fig.6 are the braking force limitations of front and rear wheels in this paper. For some special low μ road conditions such as wet and snow, the wheel locking risk generated by hard braking will be handled by ABS.

Solid blue line I joins the operating points of maximum total force for varying friction coefficient. If the front/rear wheel braking force distribution ratios always follow this blue curve, known as 'Ideal' braking force distribution ratio, vehicle will make the maximum utilization of road-tyre friction force and ensure the most stability and controllability in braking. For all load conditions, UNECE Regulations demand that the adhesion coefficient utilization curve of the rear axle must not be higher than the curve for the front axle [34,35]. With reference to Fig.6, this means that the force distribution curve should always be lower than the ideal curve.

There are lots of braking related regulations and directives from worldwide governments and organizations, but regulations in most countries are very similar to ensure that road vehicles are designed and constructed to decelerate safely and efficiently under all conditions of operation. The European UN Regulation 13-H is recognized as a valid type-approval standard in all EU and many non-EU countries, with members of the 1958 Agreement including Japan, USA, Canada, Australia, Korea, China, India, and Malaysia. It requires that, for all states of loading, two-axle vehicles that are not equipped with ABS, the rate of braking must meet the requirement of Eq.11

$$z = a/g > 0.1 + 0.85(\mu - 0.2) \quad (11)$$

Although for the weight of the vehicle assumed in the specification of Table 1.A, UN Regulation 13-H actually applies, in which the 0.85 factor in Eq.11 is replaced by 0.70, we will adopt the more demanding 0.85 factor of Regulation 13 assuming a greater margin of safety is desired. The distribution of braking forces is given by Eq.12 and Eq.13, which is shown by the golden curve in Fig.6.

$$F_{bf} = \left(L_b + zh_g\right)(z + 0.07)g/0.85L \quad (12)$$

$$F_{br} = mgz - F_{bf} \quad (13)$$

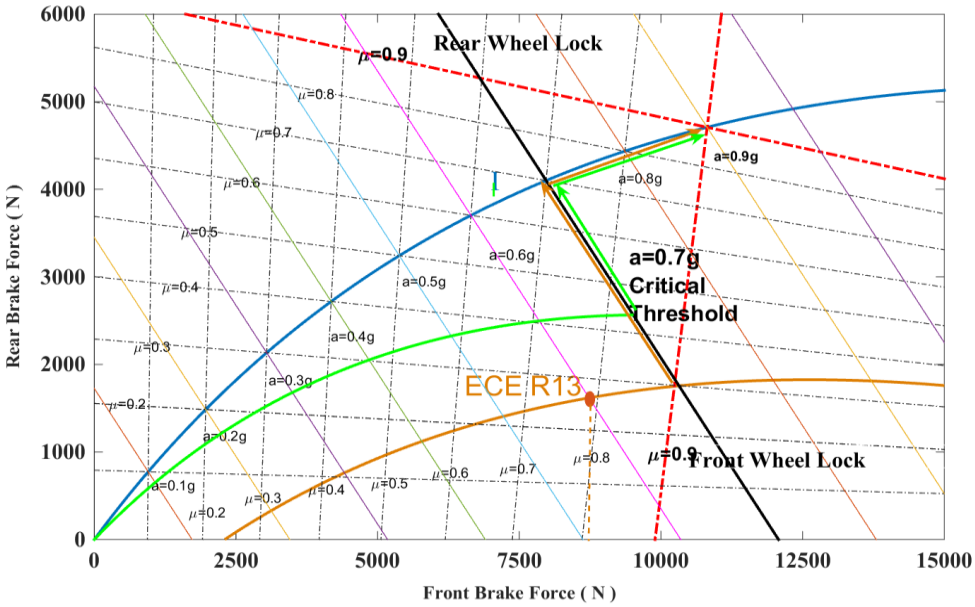

Figure 6: Braking force distribution on front and rear wheels for the vehicle of specification

In summary, the area, restricted by solid blue 'Ideal braking force distribution' curve, red dash-dot 'maximum available friction braking force on front wheels' curve, golden ECE R13-H regulation curve, and horizontal axis, indicates the range of available braking force distribution ratios of front and rear wheels.

5.3 Safety (Motor Priority) Strategy

Braking safety, including stopping distance, stability and controllability, is always the top priority and is likely to be tested by bad weather and road conditions. The motion of a wheel in a normal driving vehicle consists of two parts, namely rolling and sliding, which causes a difference between the speeds of the vehicle and the wheel. In the longitudinal direction, if the force applied to the wheel by brake calipers exceeds the maximum available friction force between the tires and ground, then the relative motion between the tires and road will change from a mix of sliding and rolling to pure sliding (Eq.3). This phenomenon is known as 'wheel lock'. Specific to the blended braking system, it occurs when the total braking force from the motor and calipers exceeds the friction force from the ground:

$$f_{regen} + f_{caliper} > f_{brake\_friction} = mg\mu \quad (14)$$

The wheel slip ratio is defined as the ratio of difference between the rotational speed of the wheel and the translational velocity of the wheel center:

$$\lambda = \Delta v / v = \left(\omega r_{dyn} - v\right)/v \quad (15)$$

ω is the wheel rotation speed and r_{dyn} represents the dynamic radius of the wheel, which is determined indirectly by measuring the travel distance per rotation circle. λ is a value from 0 to 1 representing the motion of wheel from freely rolling to lock. The solid blue curve in Fig.7 shows the dependence of the friction factor μ on the longitudinal slip ratio λ on dry asphalt pavement. The μ drops significantly when the vehicle is travelling on a wet or snow-covered road, which are presented by solid and dashed green curves . Moreover, a steering angle causes the friction factor to fall as well.

The force in the lateral direction of the road-tire contact surface directly affects the direction controllability of the vehicle. A locked wheel cannot generate lateral force to offset the sideslip trend, when cornering or unintentionally steering during an emergency brake, resulting in unnecessary under-steering and uncontrollable over-steering. As shown in Fig.7, the lateral friction factor falls dramatically with increased longitudinal braking slip ratio. For example, for a wheel with 5° steering angle and 20% longitudinal slip ratio, the lateral friction factor only equals half that of pure straight driving. When the longitudinal slip ratio hits 100% (wheel lock), steering input has no result on yaw motion because the front tires are saturated, and no lateral force can be generated. If it happens to the front wheel, the vehicle will lose steering ability. However, there is no directional instability because whenever the lateral movement of the front wheels occurs, a self-correcting moment due to the inertial force of the vehicle about the yaw center of the rear axle will be developed [36]. Consequently, it tends to bring the vehicle back to a straight line path. In contrast, if the rear wheels are locked, they lose their capability to generate the required side forces and the rear end might start to slide sideways, losing directional stability. The omitted red arrows on the rear wheel and front wheels, in the 'Over-steering' and 'Under-steering' Fig.6 schematics, indicate the locked wheels and lost lateral force. The black arrows show the potential movement directions.

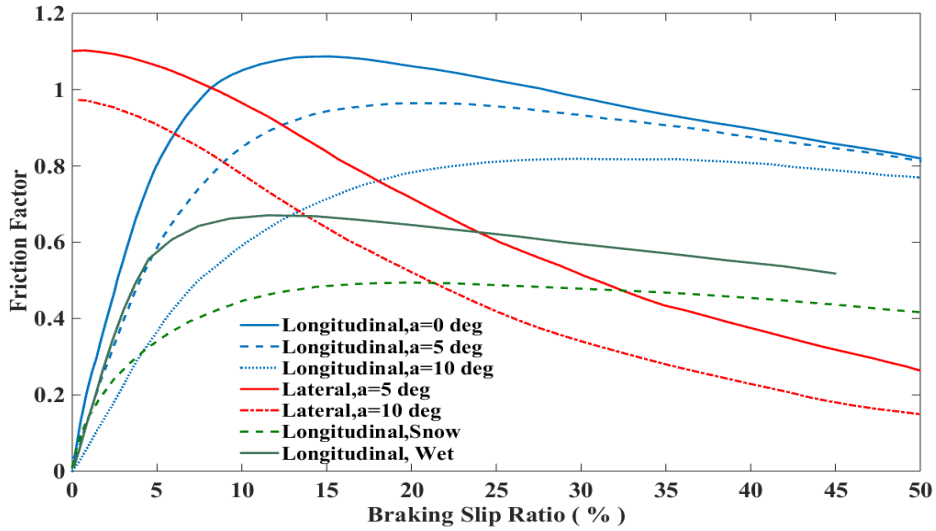

Figure 7: The influence of slip ratio, steering angle ("a" in degrees) and road condition on friction factor [37]

The most ‘Safety’ strategy should properly distribute braking force to each wheel, keeping their operating points below the maximum front and rear road friction curves (Red dash-dot bolt lines in Fig.6). Use this strategy at maximum braking all wheels lock simultaneously.

The critical threshold of deceleration rate in an emergency brake, also known as ABS activation threshold, is set as 0.7g in this paper. It is worth noting that the thresholds vary according to wet or dry road conditions. Wet road conditions trigger ABS activation when deceleration exceeds 0.65g, whereas dry road conditions trigger ABS activation when deceleration exceeds 0.90g [38]. ABS is assumed to activate if adjustable maximum deceleration thresholds are exceeded. There are two main reasons why the method used in the model to determine ABS activation was employed. For the ABS Activation condition and for emergency braking conditions that use ABS activation as triggering criteria, is simply set as 0.7g. First, this threshold is widely used in a lot of applications, testing procedures and researching reports [39–42].Second, the incidence of braking events with peak decelerations above 0.7g is relatively rare, occurring, on average, approximately once every 4800 [38].

Therefore, if the strategy is manually set to ‘Safety’, or if the deceleration rate goes over this threshold value in other strategies, then the braking force must be ideally distributed to the front and rear wheels, i.e. on the blue curve I in Fig.6, To recapture as much braking energy as possible, ‘Safety (Motor Priority)’ strategy is proposed, in which the motor takes responsibility for supplying the required front torque until reaching its maximum ability. The principal and details of this strategy are presented in Fig.9. Of course, any wheel lock occurrence would be detected and avoided by ABS. Non-ideal braking force distribution strategies result in asynchronous wheel locking time, which can cause over-steering or under-steering.

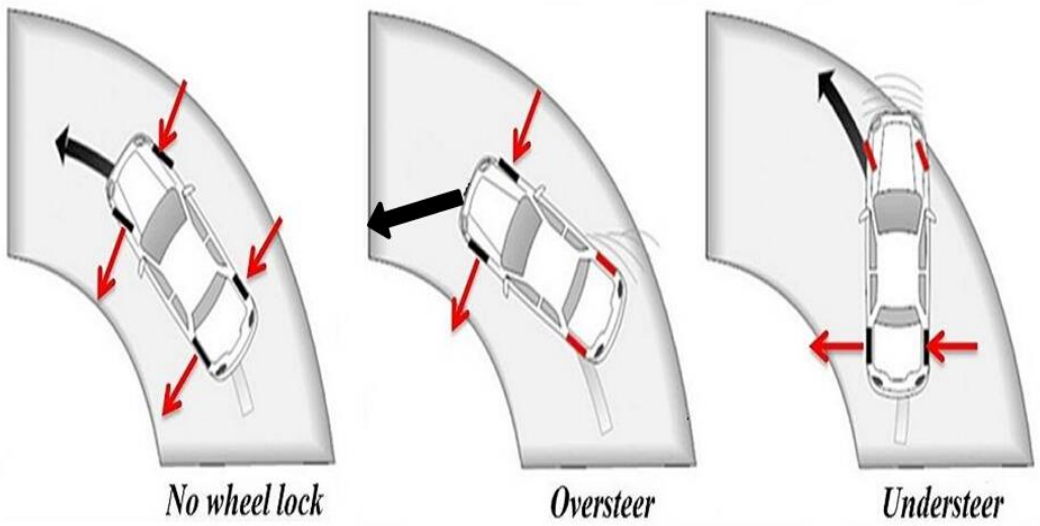

Figure 8: Schematic over-steering and under-steering when wheels lock, shown in red. Red arrows show lateral forces on unlocked wheels.

5.4 Eco Strategy

To maximize the recovery of braking energy, only the front electric brake is utilized while deceleration remains below the critical intersection point, which is determined by the horizontal axis and ECE R13-H regulation curve. After that, the ratio of front and rear axle braking force follows the ECE regulation curve, the golden one in Fig.6, until the deceleration triggers the emergency situation-0.7g. Then, the distribution strategy jumps to the 'Safety (Motor Priority)'.

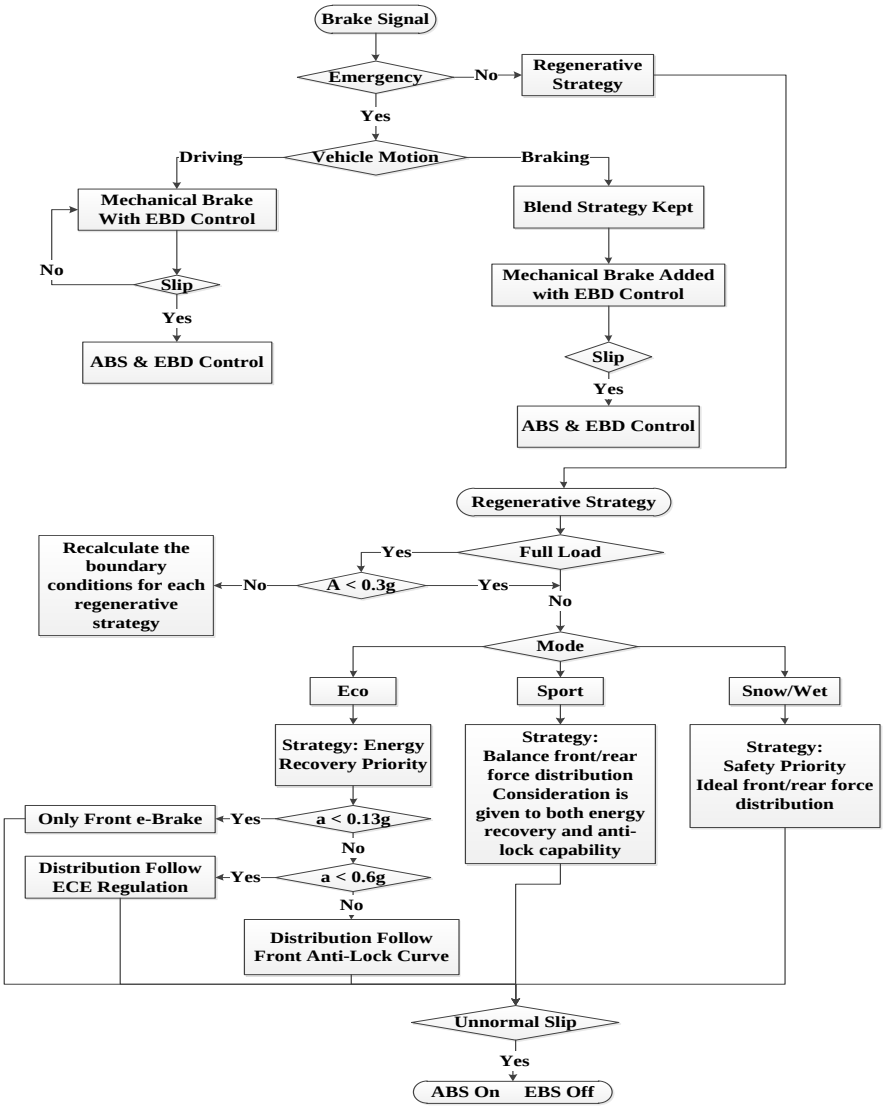

Figure 9: The Cooperation of RBS, EBD and ABS

5.5 Sport Strategy

Aggressive driving is desired when the driver intentionally selects this strategy. High acceleration and deceleration and more frequent start-stops may increase the possibility of motor failure. Therefore, any motor failure caused by the frequent and fast changed torque requirements should be avoided. This requires that the demanded motor torque never exceeds the motor ability, regardless of the motor speed and gear ratio. Because the available electric brake varies according to the motor speed and gear ratio for a full pedal brake. The minimum available electric force in a full pedal brake ($Regen_{min}$) appeals at the highest motor speed with the minimum gear ratio, which are 8000 rpm and 5.36 respectively in the specification of Table.1A. To ensure this critical value is always lower than the required electric brake, the ratio of minimum full pedal electric brake force and the theoretical maximum brake force (mu equals 1) is defined as the ratio of regenerative/total required brake:

$$\frac{Regen_{min}}{Friction_{max}} = \frac{\frac{T_{min} \times i_{g2}}{r}}{m \times g \times mu} = \frac{\frac{150 \times 5.36}{0.3125}}{1500 \times 9.81 * 0.9} = 19.4\% \quad (16)$$

Compared to the Eco strategy when electric braking has the priority and mechanical braking works as a supplement, the mechanical braking torque and the motor supplied braking torque act jointly all the time in Sport strategy. Based on the braking force distribution in Safety strategy, additional 15.8% of total required braking force is applied to the front axle, comes from motor. Consequently, if motor works well, the friction and electric braking force will increase continuously and smoothly without any braking source alternation, at a fixed ratio. If motor out of order, the mechanical braking will work alone with an 'Ideal' front/rear distribution ratio to guarantee a stable and controllable deceleration.

5.6 Motor Fault Insurance Strategy

Generally, electromagnetic equipment is considered to be not as robust as a hydraulic system. Specific to the blended braking system, motor downtime is a very dangerous situation, whether caused by IGBT failure or temperature protection. Especially during long continuous downhill braking, high current may cause motor overheating and trigger a protection mechanism, especially if the cooling system is out of order. It is not common, but is a serious event. A fail-safe provision of hydraulic braking should be activated immediately when electric braking torque is limited or a 'torque error' is detected. Including consideration of motor overload and error redundancy, a fail-safe mechanism for the motor is presented in Fig.10.

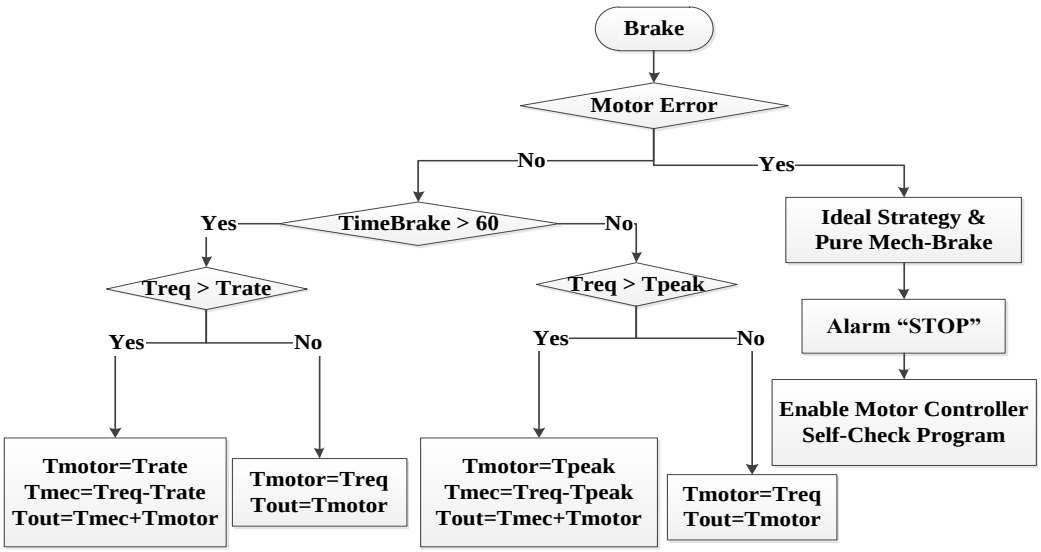

Figure 10: Motor control & fail-safe strategy

6. Brake Performance Analysis

The goal of automotive braking system design, whether for conventional or blended systems, is to achieve a comfortable and reliable deceleration at the request of the driver. In addition, the vehicle must be brought to a stop as soon as possible in an emergency situation, while maintaining dynamic stability and controllability.

6.1 Single straight line braking

In this testing profile, the vehicle begins to decelerate from 100 km/h to 92.8 km/h in 2 seconds, then, slows down to 60.4 in 3 seconds, and finally brakes to a full stop in the next 2 seconds. The deceleration increases from 0.1g (Mild Braking) to 0.3g (Moderate Braking) to 0.9g (Emergency Braking) in three stages. Fig. 9 shows the braking forces and wheel slip versus time for the different strategies introduced in Sec. 5 and Fig. 11 plots the trajectory of the distribution of braking forces to the axles for each strategy.

As shown in Fig.11 (a) and (b), the Eco strategy distributes the required braking force to the front axle as much as possible under the limitation of laws and regulations. Most of the front braking force is supplied by the motor, which is represented by the black dotted curve. During mild braking, all the required braking force is supplied by the front-wheel regenerative brake. During moderate braking, front electric braking and rear friction braking, which is represented by the red dash-dot curve, share the increased braking force demand. Finally, during emergency braking, front friction braking (blue dash curve) increases sharply to compensate for the insufficient front braking force, due to the output torque limitation of the motor. It is apparent from Fig.12 that the purple curve strategy should be switched to the safety strategy, red

hexagram curve, to avoid any wheel locking when the front or rear braking force goes over the 'wheel lock' line.

Therefore, if the strategy is not already chosen as 'Safety', the strategy should be automatically switched to 'Safety' when emergency braking occurs. The braking force distribution ratios of 'Eco' and 'Sport', represented by star and triangle curves in Fig.12, are automatically switched to 'safety' when deceleration gets close to 0.7g. As a result, both of them have satisfactory braking performance, as demonstrated by the actual speed following the target speed in Fig.11 (c) and (e). No braking force comes from the front friction brake in the 'Eco & Safety' strategy before emergency braking arises, after which the distribution ratio is switched to the 'Sport & Safety' strategy.

There is no difference between the 'Safety' and 'Safety (Motor Priority)' strategies with regard to the front/rear braking force ratio. Nevertheless, the 'Safety (Motor Priority)' strategy differs from the 'Safety' strategy by introducing braking force in series mode. Firstly, the electric brake supplies braking torque as much as possible until reaching its limitation, then, compensation is made by hydraulic friction braking on the front wheels to meet the driver's deceleration demand.

Comparing these four strategies, the safety performance of 'Eco' (no switching) strategy is the worst. It cannot stop the vehicle in a satisfied distance in an emergency case due to the wheel locking, although it can recover the most kinetic energy. Because the 'Safety (Motor Priority)' strategy always guarantees front and rear wheels lock simultaneously, it has the best safety performance and doesn't need to take the risk of strategy switching failure, like 'Eco & Safety' or 'Sport & Safety'. Furthermore, it has a higher utilization rate of electric braking than 'Sport & Safety', because the electric brake is strictly restricted to a certain level. The 'Eco & Safety' strategy has the highest energy recovery rate and an excellent decelerating stability. However, the potential risk of failure switching between two strategies demands extra attention.

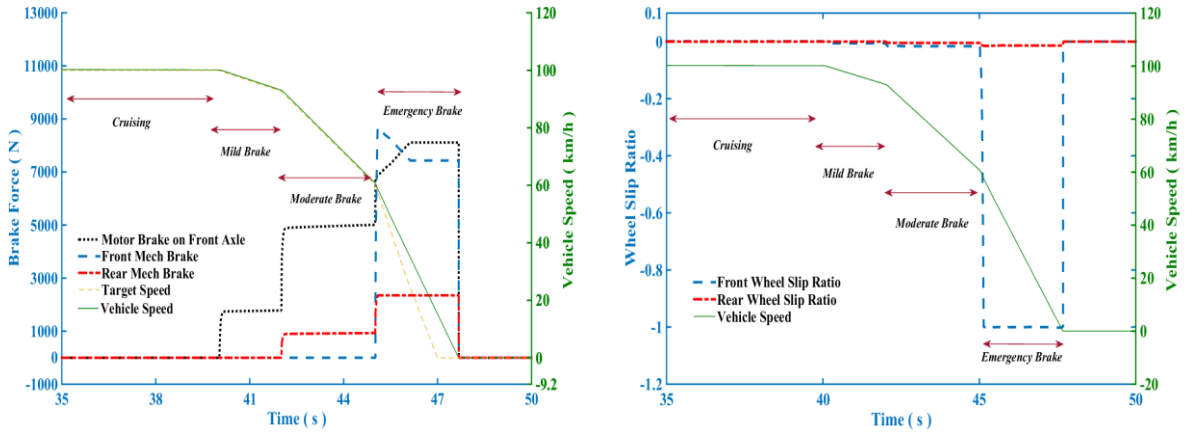

(a) Braking force distribution in Eco strategy (b) Slip ratio in front & rear wheels for (a)

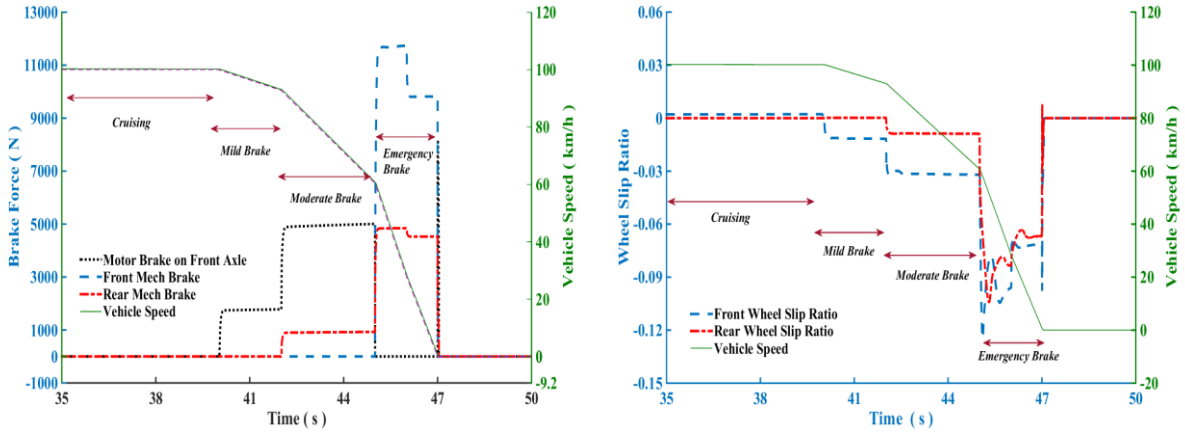

422

423 (c) Braking force distribution in Eco & Safety strategy (d) Slip ratio in front & rear wheels for (c)

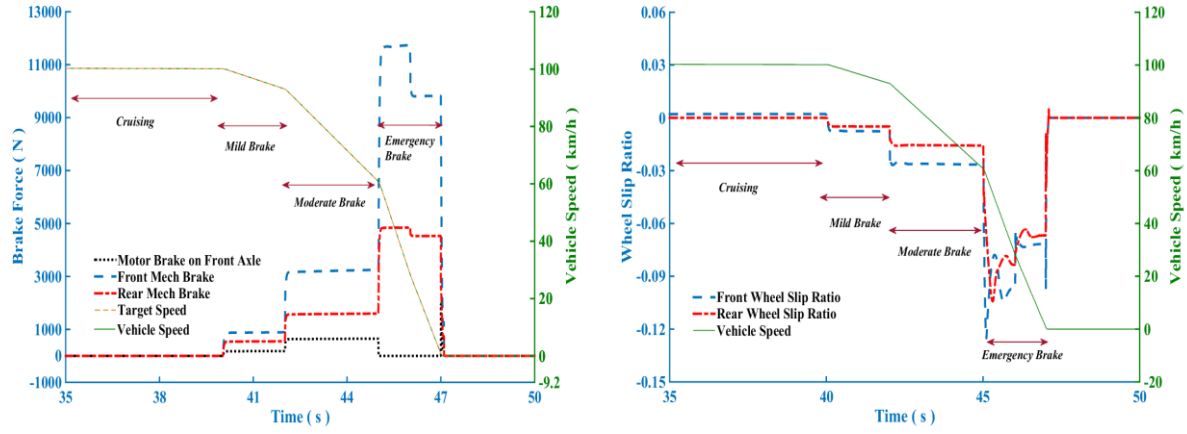

424

425 (e) Braking force distribution in Sport & Safety strategy (f) Slip ratio in front & rear wheels for
426 (e)

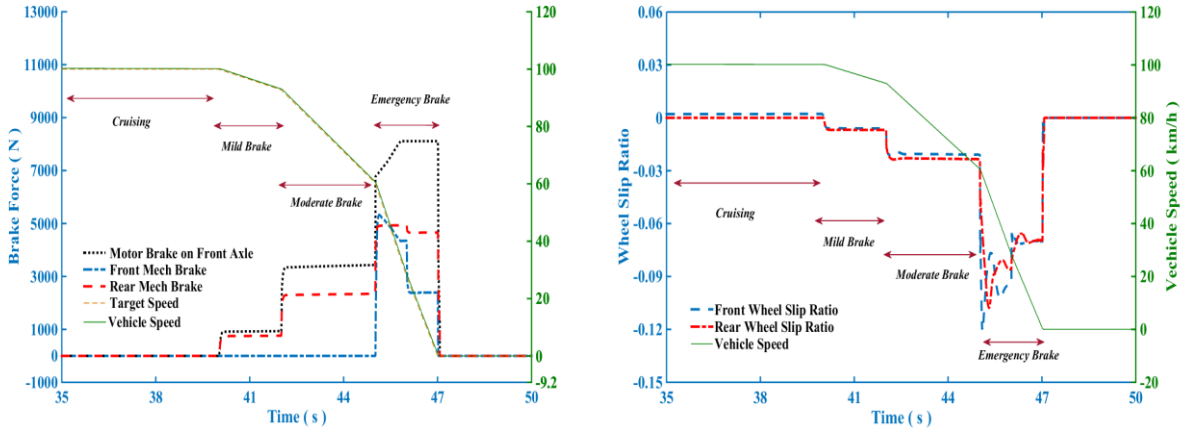

427

(g) Braking force distribution in Safety (Motor Priority) strategy (h) Slip ratio in front & rear wheels for (g)

Figure 11: Straight line braking force distribution and wheel slip ratios for: (a) and (b) Eco strategy; (c) and (d) Eco & Safety strategy; (e) and (f) Sport & Safety strategy; and (g) and (h) Safety strategy.

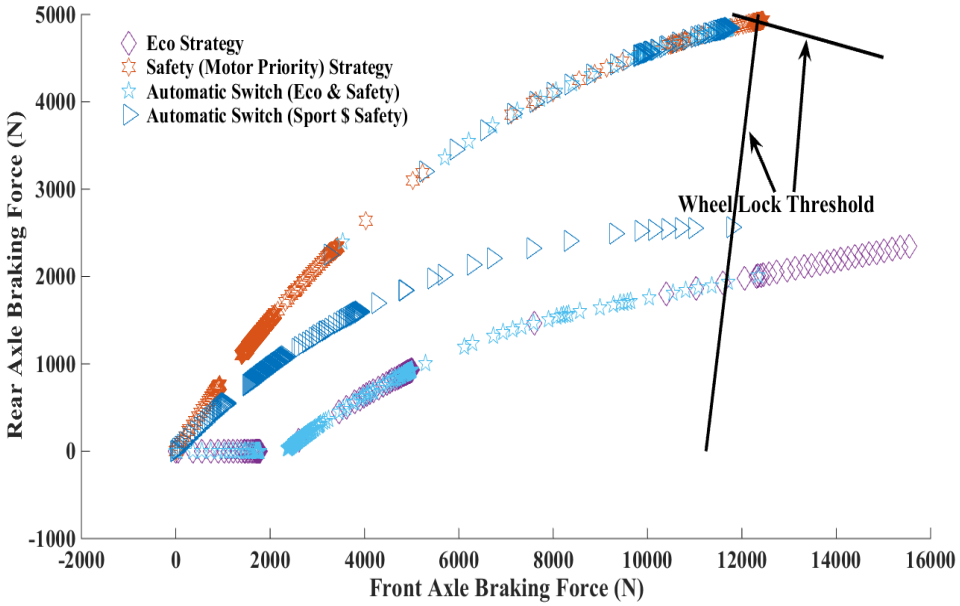

Figure 12: Front/Rear braking force distribution ratios for different strategies

6.2 The cooperation of ABS, EBD and RBS

In traditional ICE vehicles, to ensure the maximum braking force is available and to avoid wheel slipping, driver assistance systems are integrated into the vehicle such as ABS and EBD. The implementation relies on the hydraulic accumulators and actuators to work corporately with a complex relationship. In brief, the EBD supplies appropriate forces to help vehicle running on the initial intended path, while the ABS stands by ready to prevent any wheel lock. However, with an RBS seeking braking energy recovery, the strategies and intervention time of hydraulic brake systems may change.

Deceleration rates varying braking and Split Mu braking shows big challenges for blended braking strategy design. In this paper, the safety-oriented cooperation of RBS, ABS and EBD is analyzed and proposed, without going into the details of ABS or EBD.

6.2.1 RBS with EBD

When the deceleration intention is detected from the brake pedal in RBS, the motor begins to apply braking torque on the front wheels; meanwhile, pressure is established in the rear

hydraulic actuator to decelerate the rear wheels. The braking force variation on the front and rear wheels, which is usually implemented by tuning the hydraulic accumulator and actuators, now can be provided by the motor from the viewpoint of energy recovery.

Fig.13 shows how the additional load affects braking performance and how a shorter stopping distance is achieved by RBS & EBD acting jointly. The variations of braking force distribution for normal load and added load with/without EBD are demonstrated by bar indicators. According to Fig.4, EBD should distribute more braking force on the front wheel to offset the load transfer and avoid rear wheels locking. In contrast, when the vehicle is loaded with passengers or goods in back rows, EBD automatically detects and redistributes more braking force on the rear wheels to utilize the increased available friction force, as demonstrated in Fig.13-2A. However, the real distribution ratio is kept as the previous one from the viewpoint of energy recovery, instead of increasing rear braking force and reducing front braking force immediately, at the cost of a longer stop distance (Fig.13-2B). However, this only happens in mild braking ($a<0.3g$). Stopping distance becomes the top concern when braking intention is detected stronger ($a>0.3g$). The braking force distribution is rebalanced to take full advantage of load transfer. Rear mechanical braking force is increased, at the same time, reducing front mechanical braking and keeping motor braking, or reducing motor braking if there is no mechanical brake on the front wheels. The rebalance and detection procedures are described in the flowchart (Fig.9).

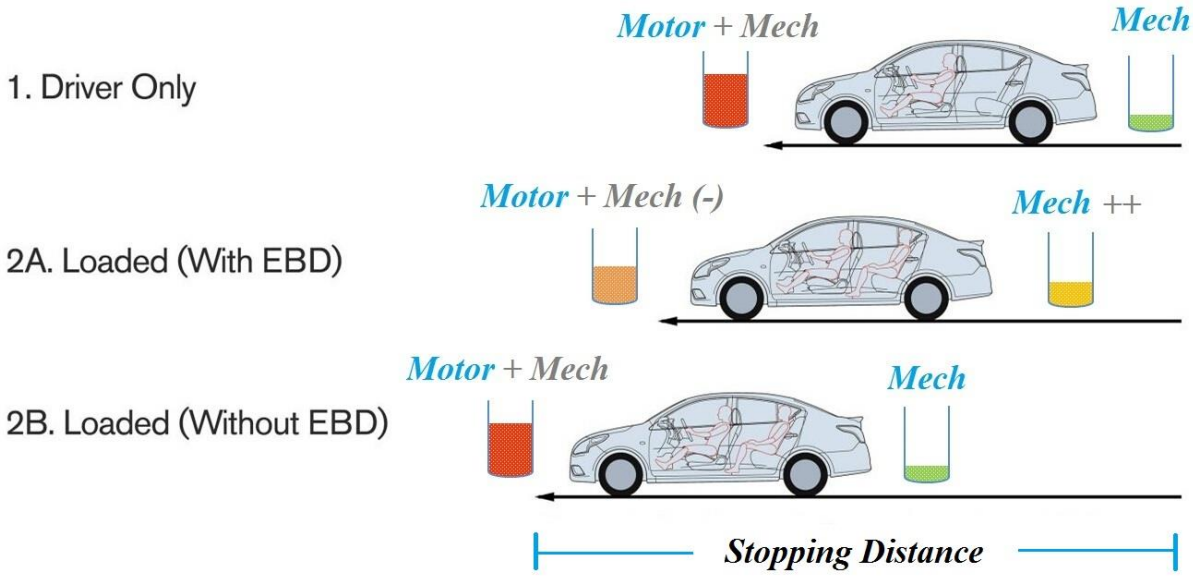

Figure 13: RBS Cooperate with EBD

6.2.2 RBS with ABS

ABS becomes involved when emergency braking is activated. ABS reduces the pressure in the hydraulic brake actuator of the wheel that is tending to lock. However, there are two different preconditions for the blended braking system when ABS operates:

1. Emergency braking starts from driving
2. Emergency braking starts from an existing braking event

In case 1, emergency braking usually needs a great deal of force. Using RBS alone would generate high instantaneous current in the motor, which can't be taken by the battery. Given HBS has higher reliability, hydraulic ABS is given the highest priority, which means motor braking does not participate in emergency braking in this situation.

In case 2, there is already some level of regenerative braking before the braking turns to strong. With respect to safety, keeping the existed regenerative braking and using mechanical braking to supply the rest of required braking force is the best choice. The detail of this strategy and the testing result is included in Fig.9 and Fig.14.

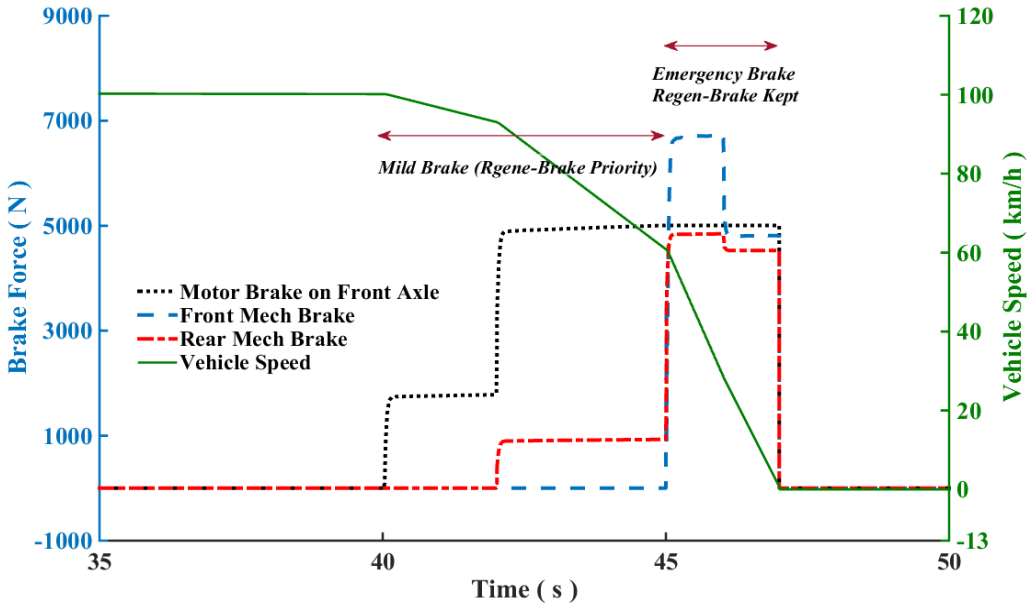

Figure 14: Emergency braking force distribution when motor torque is kept

6.3 Gear Shift during Braking

Unlike the conventional HBS, in which the braking force goes from the brake pedal to master cylinder, hydraulic actuator, and calipers, then, directly to the wheels, electric braking goes through transmissions and differentials, then acts on the driven half shafts, which are connected to each wheel. On the one hand, regenerative braking from the motor may be

insufficient when the vehicle is running at high speed with smaller gear ratio, as shown in Fig.5. On the other hand, the torque interruption introduced by gear shifting can result in a serious potential safety issue, especially for emergency braking. Although the interruption, also known as 'shifting torque hole' (Fig.15), is very short in DCT, it can still be felt and can send the wrong message to the drivers, which may cause them to take unnecessary corrective measures. Theoretically, there are two potential solutions:

1) Lock out the shifting function and use the mechanical brake to supply the rest of the required braking force;

2) Use mechanical braking to supply the reduced torque during shifting, but reinstate the motor braking torque after shifting.

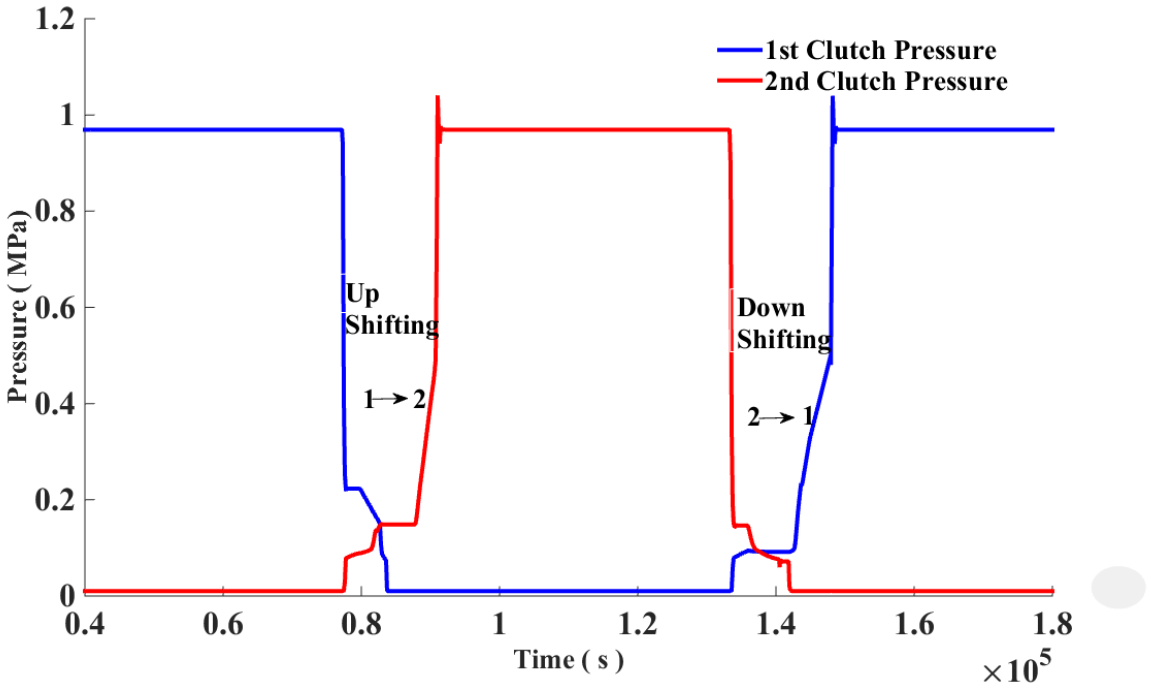

Figure 15: Clutch pressure variation during shifting

Obviously, the second solution can recapture more braking energy by giving regenerative braking more opportunities to participate. However, it also needs a more complicated control algorithm and a higher precision in monitoring of HBS and RBS. When the shifting requirement occurs in emergency braking, considering the safety risk and energy recovery potential from emergency braking over a short period, solution 1 is the favored choice for market products. However, when the shifting requirement occurs in long-downhill road with a moderate braking, a downshifting should be allowed to increase the energy recovery rate.

6.4 Braking in Typical Cycles

The following chart, Fig.16, demonstrates the braking force distribution on the front (friction & regenerative braking) and rear wheels in different strategies. The various distribution ratios result in some fluctuations of total braking force for strategies in each driving cycle.

For the 'Eco' strategy, the required braking force in NEDC, HWFET and JP1015 never exceeds the threshold of ECE R-13 regulation, so all the braking force is supplied by the motor. The two US city cycles, UDDS and LA-92, have a more aggressive braking event, and both need rear friction braking to meet the requirement of ECE R-13.

The 'Sport' strategy deliberately limits the motor's braking ability to a safe and low level, as described in Sec 5.4. Consequently, the front and rear mechanical friction braking accounts for most of the braking, rather than regenerative braking, in all driving cycles.

The motor has the priority and sufficient ability in the 'Safety (Motor Priority)' strategy to meet the front axle braking force requirement, causing a higher utilization rate of regenerative braking. Meanwhile, the lowest likelihood of wheel locking is guaranteed by the 'Ideal' braking force distribution ratio. Friction braking on the front wheels plays no role in typical driving cycle deceleration in this strategy. Because motor has the sufficient ability to meet the total front axle braking force requirement.

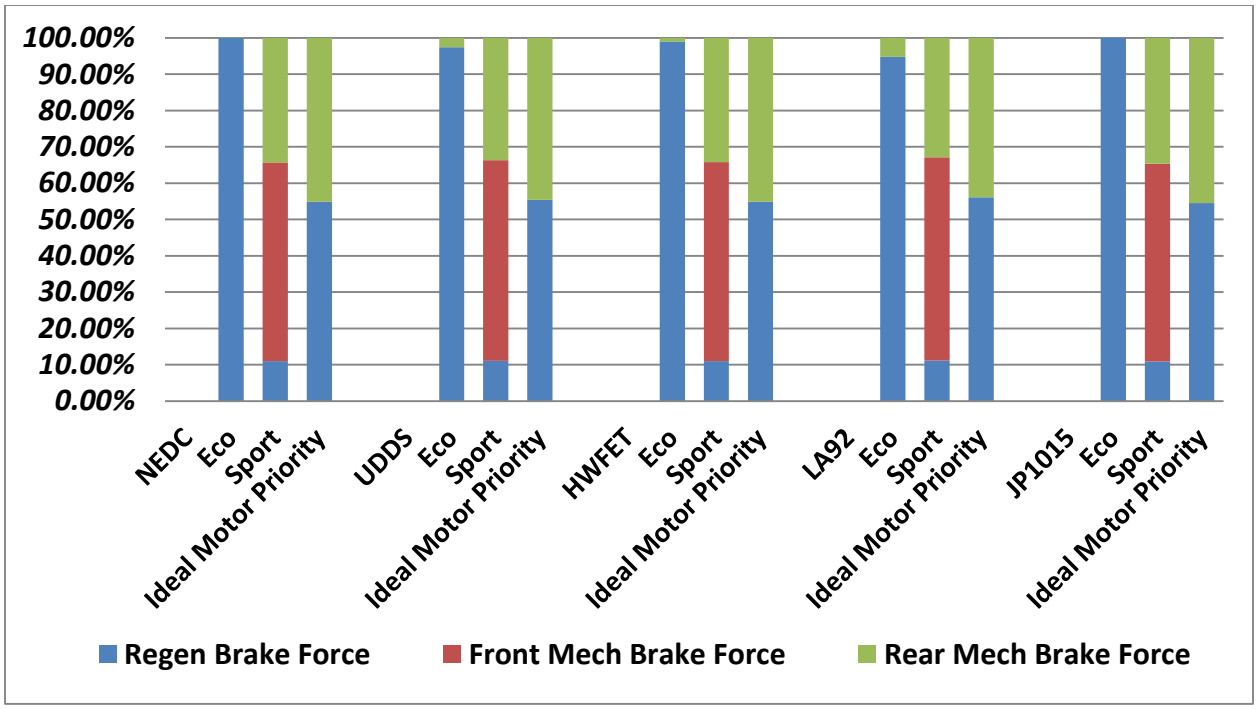

Figure 16: Braking force distribution for strategies in driving cycles

Eq.17 is used to evaluate the the braking energy recovery potential of strategies. The comparison of potential braking energy recovery rates in driving cycles is present in Fig.17. Thanks to the bigger capacity of motor and battery in BEV, comparing to HEV, and the moderate driving cycles, most of braking requirements can be covered by motor alone in 'Eco & Safety' strategy. Consequently, the energy recovery rates in this strategy are almost 100%, except some higher deceleration braking events in UDDS, LA92, and HWFET needing a complementary friction braking. Subject to the distribution ratio of front and rear braking force in 'Safety (Motor Prioirty)' strategy, energy recovery rates of different cycles are all around 55%. Regarding to Fig.16, motor supplies all the required braking force on front axle. 'Sport & Safety' strategy achieves the highest motor failure tolerance at the cost of lowest energy recovery rates, 10% for all the cycles.

$$Energy\ Recovery\ Rate = \frac{Regenerative\ Braking\ Energy}{Total\ Braking\ Energy} \quad (17)$$

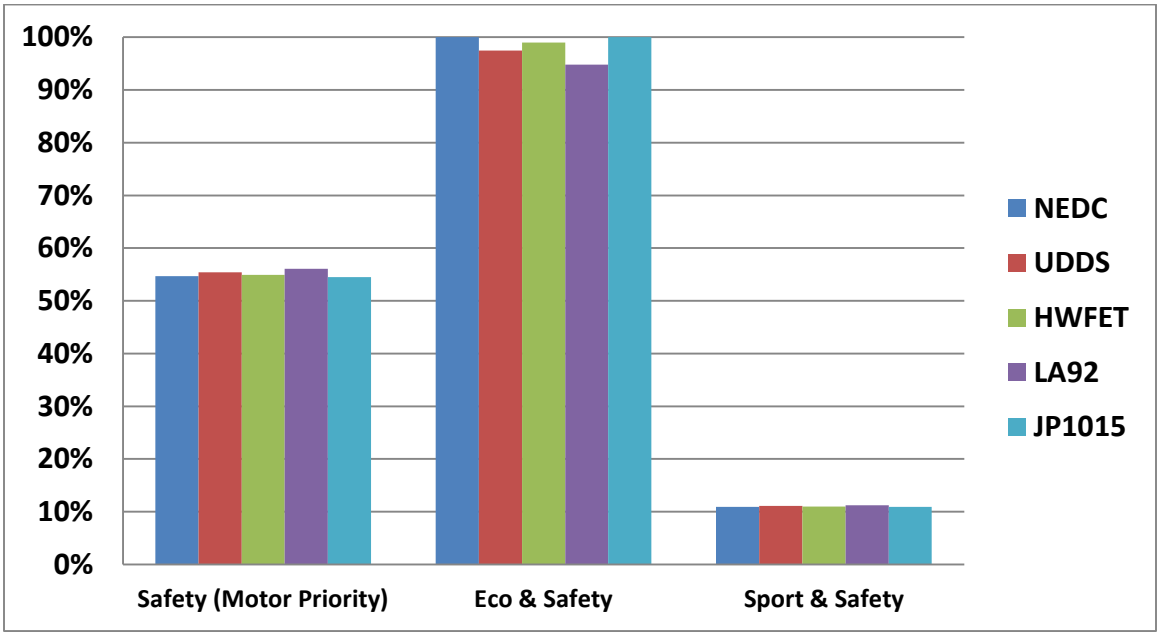

Figure 17: Braking energy recovery potential of strategies in each cycle

In the industry, battery energy recovery rate is widely accepted as the evaluation criterion of the regenerative braking system. The rate is defined as the ratio of the battery input energy from braking and the battery output energy for driving:

$$Q_{re} = \frac{E\_bat_{IN}}{E\_bat_{OUT}} \quad (18)$$

Table 1 shows a comparison of energy recovery rates for different driving cycles. Comparing the driving cycles, in columns, one observes that more energy can be recaptured in aggressive city cycles, UDDS and LA92, than others. The reason JP1015 has the highest recovery rate is that the required driving energy is bigger, compared to the recovered energy from braking. On the contrary, the recovery rate of HWFET is the lowest one.

Table 1: Energy recovery rates in term of driving cycles, plus motor failure tolerance, with + indicating a higher tolerance

Energy Recovery Rates	NEDC	UDDS	HWFET	LA92	JP1015	Controllability Lost Risk
Safety (Motor Priority)	12.4%	16.4%	8.6%	15.0%	17.8%	0
Eco & Safety	25.3%	30.4%	16.0%	24.6%	32.9%	0
Sport & Safety	2.4%	3.1%	1.8%	3.6%	3.6%	++

Comparing the strategies, in rows, safety risk is included to demonstrate a general evaluation of wheel locking possibility. 'Safety (Motor Priority)' is the baseline and has the highest avoidance of wheels lock. The highest energy recovery rate is achieved in 'Eco' because the required braking force rarely reaches the threshold of ECE R-13(H) regulation in all testing cycles, in other words, braking is supplied by the motor alone for most of the time. However, as more braking force is distributed to the front axle, the front wheels' locking point will arise earlier. Safety-oriented Sports strategy results in much lower energy recovery rate, all under 4%, due to the fixed ratio of front friction and regenerative braking.

Summarizing the strategies' performance, 'Eco' is the winner for energy recovery, although it has an earlier wheel lock threshold and higher risk of insufficient motor braking torque. 'Sport' mode can keep the vehicle decelerating as demanded, no matter what the motor speed and gear number, or even a motor fault happens. However, the braking energy recovery rate is the lowest. 'Safety (Motor Priority)' has an excellent braking performance in terms of wheel locking, and at the same time, has a satisfactory energy recovery rate.

7. Experimental Results

The integrated powertrain-testing rig incorporates a BLDC motor and controller, a differential included two-speed DCT, wheels, flywheels and a dynamometer, as shown in Fig.18. The motor is a UNIQ UQM_PowerPhase125 with ratings as given in Table 1.A in the Appendix. The UNIQ UQM_PowerPhase125 motor controller is supplied by a custom-built 380 V DC supply, which is bidirectional, i.e. can supply or absorb power. A 380 V, 72 Ah battery bank is to be also installed [43]. Its energy capacity of 20 kWh can be considered typical of a BEV. The vehicle inertia is

supplied by four flywheels in the testing rig to simulate a 1500kg whole vehicle mass. This inertia stores kinetic energy in the flywheels, simulating a road vehicle driving at some linear speed. By using these flywheels the dynamic behavior of the vehicle can be simulated accurately in a controlled laboratory. Additional external resistance force, such as dynamic aerodynamic drag and roll resistances in the driving cycles, is generated by an eddy current dynamometer. HWFET and NEDC cycles are selected in this study to consist of a combined driving cycle to simulate consumers' daily driving conditions.

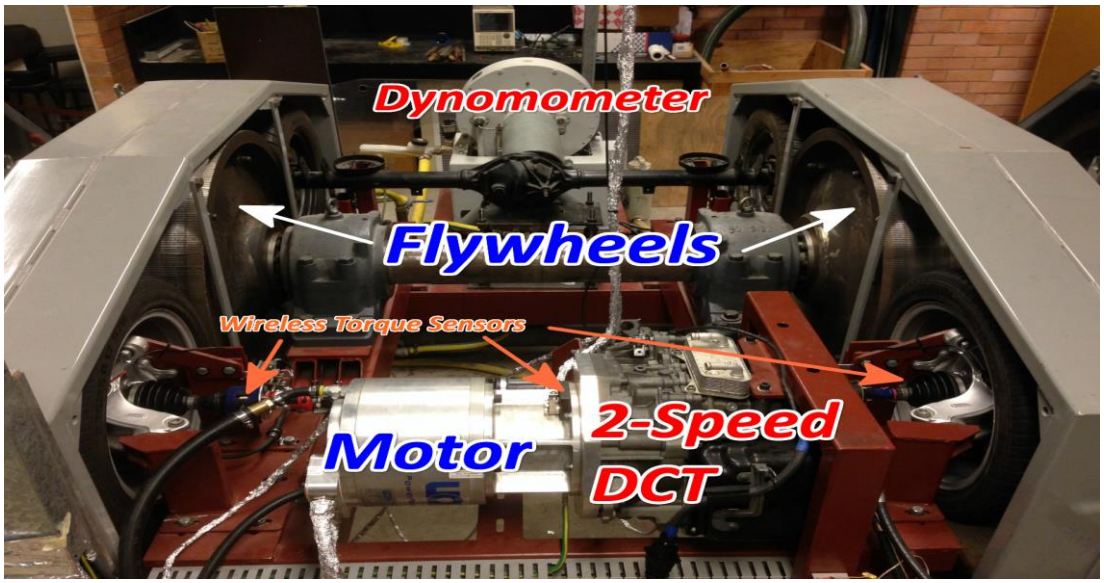

Figure 18: Vehicle powertrain testing rig

The maximum decelerations in different driving cycles are presented in Table 2. The highest deceleration, 2.2 m/s^2 = 0.22g appearing in the LA-92 cycle, is far from the wheel-lock deceleration thresholds, represented by the two red dotted curves in Fig.6. Therefore, RBS can theoretically meet all the braking force requirements. Aiming at studying the energy recovery maximum potential and testing the motor braking safety performance, 'Eco' strategies are selected in these two cycles to be experimentally validated.

Table 2: Maximum deceleration in typical driving cycles

	NEDC	UDDS	JP-1015	HWFET	LA 92
Max Deceleration (g)	0.1	0.093	0.067	0.14	0.22

As shown in Fig.19, the vehicle can be decelerated and stopped as required by regenerative motor braking alone in both cycles. The negative current generated by the motor (acting as a generator) never exceeds 90 Amps. Therefore, according to the specifications of 72 Ah battery

[43], which has maximum charging current more than 180 Amps, this charging current can be easily absorbed.

a) b)

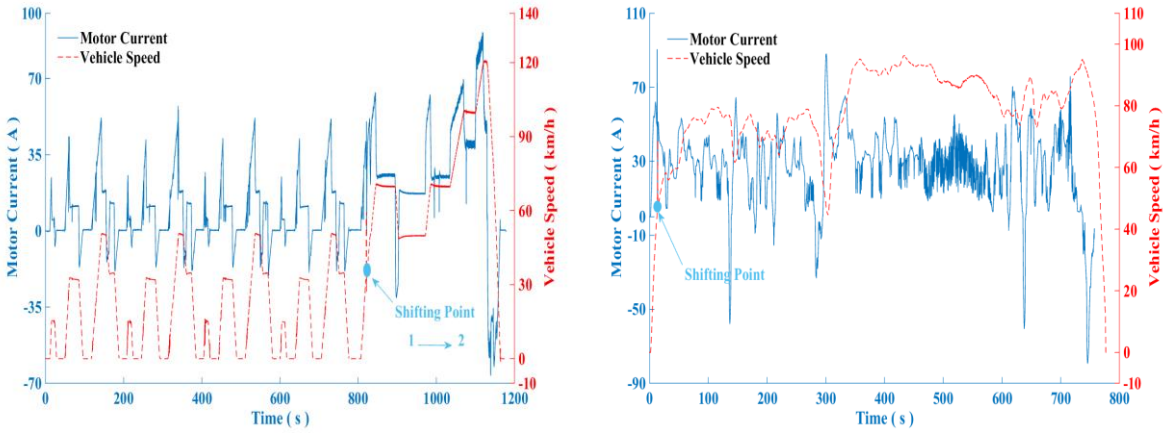

Figure 19: Motor current and vehicle speed for 'Eco' mode in: a) NEDC and b) HWFET cycles

Fig.20 & Fig.21 compare the SOC for the powertrain with and without the regenerative braking in one NEDC or HWFET cycle. We can see that the motor has sufficient ability to meet the requirement of normal braking in daily use. Significant benefits, 23.3% and 14.1% energy recovery rates for NEDC and HWFET respectively, are achieved by inclusion of regenerative braking in the 'Eco' strategy experimental testing.

a) b)

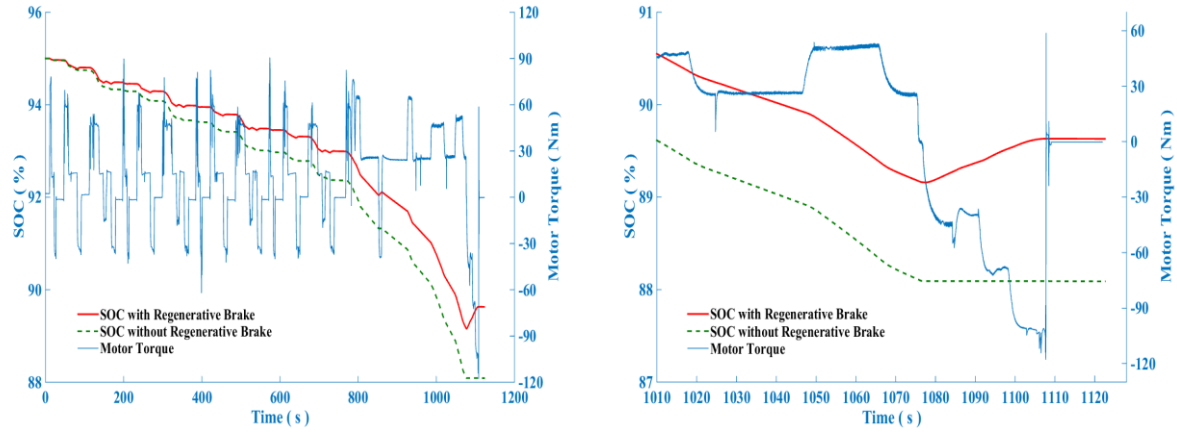

Figure 20: SOC and motor torque in NEDC cycle for 'Eco" mode over: a) the full cycle; and b) the final 100 s

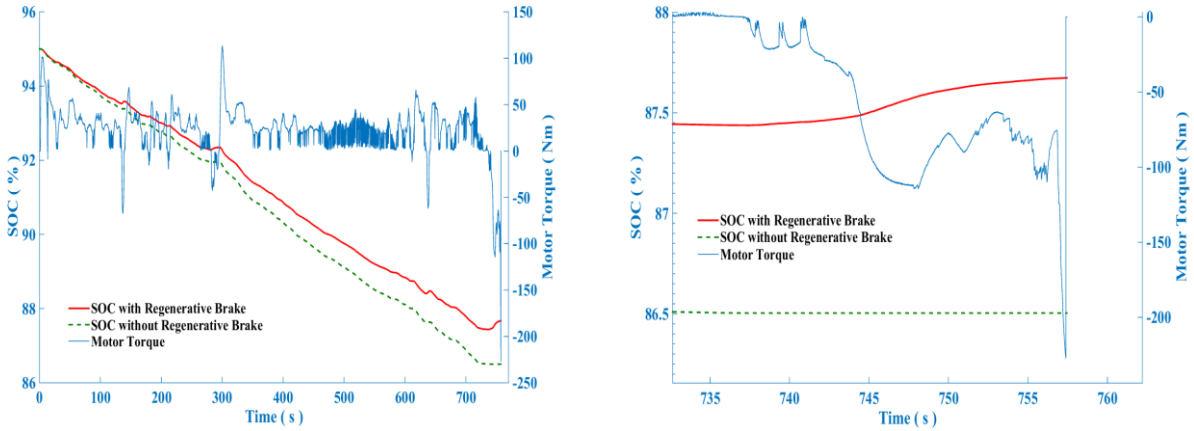

Figure 21: SOC and motor torque in HWFET cycle for 'Eco' mode over: a) the full cycle; and b) the final 25 s

8. Energy Recovery and Cost Saving Analysis

8.1 The cost saving in braking energy recovery

According to the test results in Sec.7 and the battery specification in Table.1A (Appendix), the recaptured braking energy in one NEDC and HWFET cycle by 'Eco & Safety' strategy are calculated and shown in Table.3. The measured battery energy recovery rates were approximately 10% below the simulated rates given in Fig.1, which can be considered good agreement.

Table 3: Recovered braking energy and mileage per NEDC and HWFET cycle

	NEDC	HWFET
Mileage per cycle (MPC)	11.0 km	16.5 km
Consumed energy (with no regenerative braking)	1.888 kWh	2.326 kWh
Consumed energy per km (CPK)	0.1716 kWh/km	0.141 kWh/km
Recaptured energy in braking by 'Eco & Safety'	0.44 kWh	0.328 kWh
Recovered braking energy per km (RPK)	0.04 kWh/km	0.0199 kWh/km
Battery energy recovery rate Q_{re}	23.3%	14.1%

Daily driving conditions are mixed for commuters. A particular testing cycle may have a good braking energy recovery rate but may not reflect the real performance correctly [44]. Therefore, a combined driving cycle is special designed, according to the requirement of Environment Protection Agency (EPA) of United States, to make the testing more authentic and reliable in this study. The combined cycle combines the city and highway cycles, i.e. NEDC and HWFET, with 43% and 57% weightings for the distance spent in each cycle respectively [45] [ref]. The reasonable consumed and recaptured braking energy per km of a combined driving, i.e. $CPK_{Combined}$ and $RPK_{Combined}$, are shown in Eq.19 and Eq.20, comparing to $0.12\ kWh/km$ in an average cycle and ranging from $0.1 - 0.16\ kWh/km$ for individual cycles [46].

$$CPK_{Combined} = \frac{1}{\frac{0.57}{CPK_{HWFET}} + \frac{0.43}{CPK_{NEDC}}} = \frac{1}{\frac{0.57}{141.0} + \frac{0.43}{171.6}} = 0.1527\ kWh/km \quad (19)$$

$$RPK_{Combined} = \frac{1}{\frac{0.57}{RPK_{HWFET}} + \frac{0.43}{RPK_{NEDC}}} = \frac{1}{\frac{0.57}{19.9} + \frac{0.43}{40}} = 0.0254\ kWh/km \quad (20)$$

The total mileage per charge for EV without regenerative braking is:

$$Range_{without\_Regen} = \frac{C_B \times V_B}{CPK_{Combined}} = \frac{72 * 380}{152.7} = 179.2\ km \quad (21)$$

The total mileage per charge with regenerative braking is:

$$Range_{with\_Regen} = \frac{C_B \times V_B}{CPK_{Combined} - RPK_{Combined}} = \frac{72 * 380}{152.7 - 25.4} = 215\ km \quad (22)$$

Therefore, the rate of extended mileage per charge with same battery for vehicle equipped with regenerative braking is:

$$Extended_{Mileage_{Rate}} = \frac{Range_{with\_Regen} - Range_{without\_Regen}}{Range_{without\_Regen}} = 20.0\% \quad (23)$$

In term of battery capacity, the reduced requirement for the same travel distance, 188 km, is:

$$C_{reduced} = Range_{without\_Regen} \times RPK_{Combined} = 188 \times 25.4 = 4.8\ kWh \quad (24)$$

The energy consumed per 100 km with and without regenerative braking respectively in specification Table 1A are:

$$No\ Regen: 152.7\ \times 100 = 15.27\ kWh \quad (25)$$

$$Regen: (152.7 - 25.4) \times 100 = 12.73\ kWh \quad (26)$$

Fig.22 clearly demonstrates the braking energy recovery benefit, regarding to the driving range improvement and energy consuming minimizing. Top left three points, representing BEV with regenerative braking, have a longer driving range per charge and lower energy consuming rates (kWh/100 km), comparing to bottom right three points without energy recovering. Specific to cycles, highway cycle has the best performance, and city cycle consumes more energy. This graph also validates the effectiveness of representing two different kinds cycles for combined cycle.

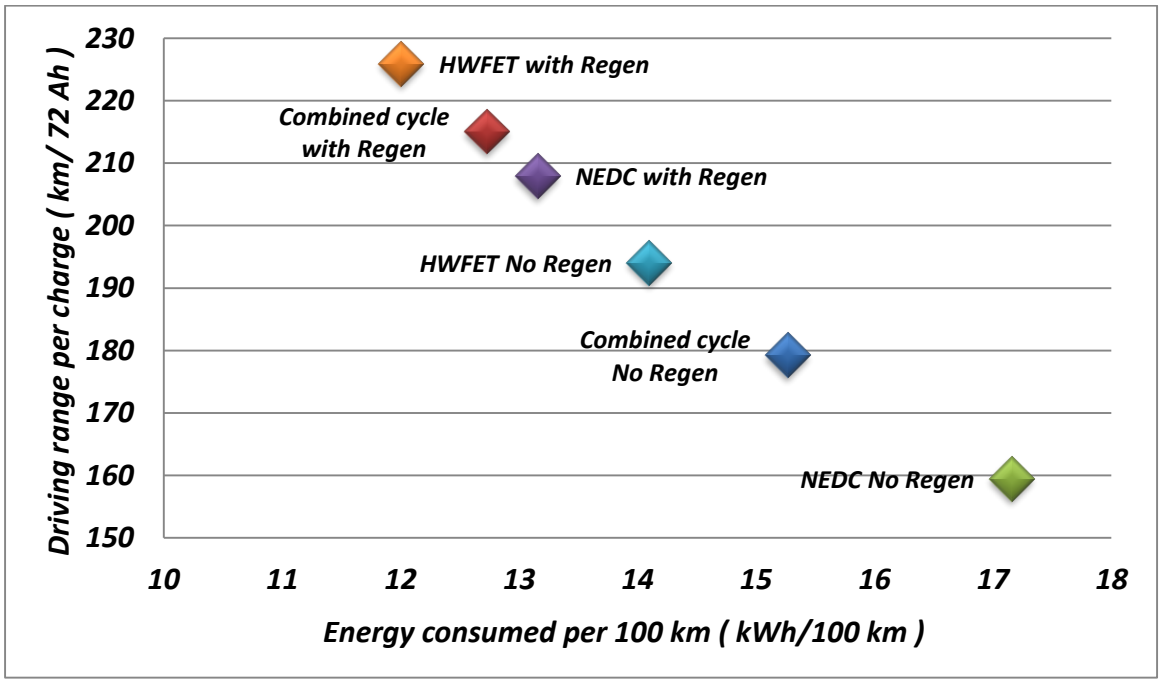

Figure 22: Driving range and energy utilization benefit of braking energy recovering

A typical passenger vehicle will travel a lifetime mileage of 250000 km according to [47] or 208000 km according to the product of the typical annual average travel of 18240 km per year [48] times the typical 11.4 years average vehicle life [49]. Considering that the powertrain of an EV is more reliable and simpler than that of the traditional vehicle, having a more robust motor and no gearbox or a simple 2-3 speed gearbox, 250000 km lifetime mileage is taken in this paper. Additionally, the charging efficiency with Level 2 standard voltage is 81% [50], as a result of same 90% efficiency for both plug-in charger and lithium-ion battery charge/discharge [51]. The total expected electricity energy saved by regenerative braking with 'Eco' strategy in the whole life cycle is:

$$E_{save} = \frac{RPK_{Combined} \times Range_{lifetime}}{Charging\ Eff} = \frac{0.0254 \times 250000}{0.81} = 7840\ kWh \quad (27)$$

651 Since the limited electricity energy in the battery can be replenished by regenerative braking,
652 significant cost saving can be achieved by reducing the required capacity of this expensive
653 power source. The prices given in Table 4 are based on data and results from laboratory and
654 industry [52–55]:

655 Table 4: Manufacturing cost and retail price of EV basic parts

Vehicle component	Cost (US $)
Battery manufacture	**$ 400/kWh**
BMS, power electronics, etc.*	**$ 238/kWh**
Battery pack final cost (incl. margin and warranty)	**$ 800/kWh**
Average electricity cost (in Australia)	**$ 0.3/kWh**

656 *This part includes battery management system (BMS), power electronics, connections, cell
657 support, housing and temperature control.The estimated battery charge/discharge cycles in
658 vehicle lifetime span with deep (80%) / swallow (45%) depth of discharge (DOD) are calculated
659 in Eq.28 and Eq.29:

$$Without\ Regen\begin{cases} LifeCycle_{50\%DOD} = \dfrac{250000/100 \times 15.27}{72 \times 380/1000} \times \dfrac{1}{50\%} = 2791 \\ LifeCycle_{80\%DOD} = \dfrac{250000/100 \times 15.27}{40 \times 380/1000} \times \dfrac{1}{80\%} = 1744 \end{cases} \quad (28)$$

$$With\ Regen\begin{cases} LifeCycle_{50\%DOD} = \dfrac{250000/100 \times 12.73}{40 \times 380/1000} \times \dfrac{1}{50\%} = 2326 \\ LifeCycle_{80\%DOD} = \dfrac{250000/100 \times 12.73}{40 \times 380/1000} \times \dfrac{1}{80\%} = 1454 \end{cases} \quad (29)$$

660 The reduced charging/discharging cycles in different DOD by regenerative braking are:

$$\begin{cases} LifeCycleSave_{50\%DOD} = 2791 - 2326 = 465 \\ LifeCycleSave_{80\%DOD} = 1744 - 1454 = 290 \end{cases} \quad (30)$$

661 The lifetime cycles of a typical li-ion battery are 3200 and 18000 for deep and swallow DOD
662 respectively at room temperature (25°C) [56]. However, the lifetime cycles are not only related

to DOD, also subjected to operating temperature and chemical materials. With the increasing working temperature, higher DOD and discharging rate, the life cycles declines to lower than 1000 [57–59]. Additionally, considering the 5-8 years battery calendar year life span[57,60,61], it is inevitable for battery EV to replace the battery pack at least one time during the whole vehicle life. There is no doubt that regenerative braking can improve the battery life in terms of cycles/calendar year aging, however, the reduced charging/discharging cycles are not enough to save a whole battery pack.

In summary, the costs saving in electricity fee and battery pack by 'Eco' strategy are:

$$Electricity_{save} = 7840 \times 0.3 = 2352\ (USD) \quad (31)$$

$$BatteryPack_{save} = 800 \times 4.8 = 3840\ (USD) \quad (32)$$

8.2 The cost saving in braking equipment maintenance

Comparing to the mechanical parts in traditional vehicles, electrical components such as traction motors require little maintenance. The estimated overall maintenance costs for a BEV is approximately 70% of an equivalent ICE vehicle [62]. Specific to the RBS, the unique advantage is the durability and high-temperature resistance compared to friction braking system. Whatever the materials selected for brake disk and pad, wear and deformation are inevitable, and failure is a fatality risk. Motor electric braking eliminates all these potential risks by directly applying negative torque on rotating shafts.

Depending on the vehicle type, brake pad materials, driving routes and operating environment, the average pad life varies from 28400 km to 33800 km [63]. Considering the emergency braking produces more wear than usual, ten brake pad replacements for whole 250000 km vehicle life is regarded as a reasonable assumption in this paper.

The cost of brake pads and rotors, which are presented in the following table, can be obtained from quotes on the web [64,65]. The rotors can last 2-3 sets of pads before needing replacement. The share of friction braking and motor braking for 'Sport' and 'Safety (Motor Priority)' strategies are roughly 15/85 and 50/50, based on the Fig.16 and Eq.17, which are used to calculate the required brake pads/rotors and cost respectively. Additionally, one extra pair of brake pads are added to each blended braking strategy for emergency braking.

Table 5: Friction brake applications and pedal replacement cost (US $)*

	Friction brake only	'Eco'	'Safety (Motor Priority)'	'Sport'
Number of replaced pads	10	1	6	9

Pads cost with labor (8 sets, two axles, $ USD)	$ 350	$ 350	$ 350	$ 350
Lifetime pads replacement cost	$ 3500	$ 350	$ 2100	$ 3150
Number of replaced rotors	4	0	2	3
Rotors cost with labor (4 sets, two axles)	$ 210	$ 210	$ 210	$ 210
Lifetime rotor replacement cost	$ 840	0	$ 420	$ 630

690 *Average value is used based on the reference data

691 Finally, the total cost of BEVs based on different braking architectures and strategies are
692 demonstrated in Table.6:

693 Table 6: Blended braking system related EV lifetime cost saving summary (US $)

	Friction Brake Only	'Eco'	'Safety (Motor Priority)'	'Sport'
Electricity Fee	$ 14139	$ 11787	$ 12963 (Approx.)	$ 13786 (Approx.)
Battery Pack	$ 21888	$ 18048	$ 19968 (Approx.)	$ 21312 (Approx.)
Brake Pads	$ 3500	$ 350	$ 2100	$ 3150
Brake Rotors	$ 840	0	$ 420	$ 630
Total	$ 40367	$ 30185	$ 35451	$ 38878

694

695 The effectiveness of 'Eco & Safety' strategy is validated in both city and highway cycles in this
696 experiment, expect rare emergency braking. Therefore, the 'Eco & Safety' strategy' can be used
697 to evaluate the economic benefit of regenerative braking in daily commuting, comparing to
698 conventional friction braking. The economic benefit of different blended braking strategies is
699 shown in Fig.23, regarding to 'fuel' cost and mechanical maintenance cost. As shown in Fig.23,
700 more than one fourth of total cost, including brake system maintenance and electricity, can be
701 saved by braking energy recovering in 'Eco & Safety' strategy. The figures for 'Safety (Motor
702 Priority)' and 'Sport & Safety' are 12% and 4% respectively.

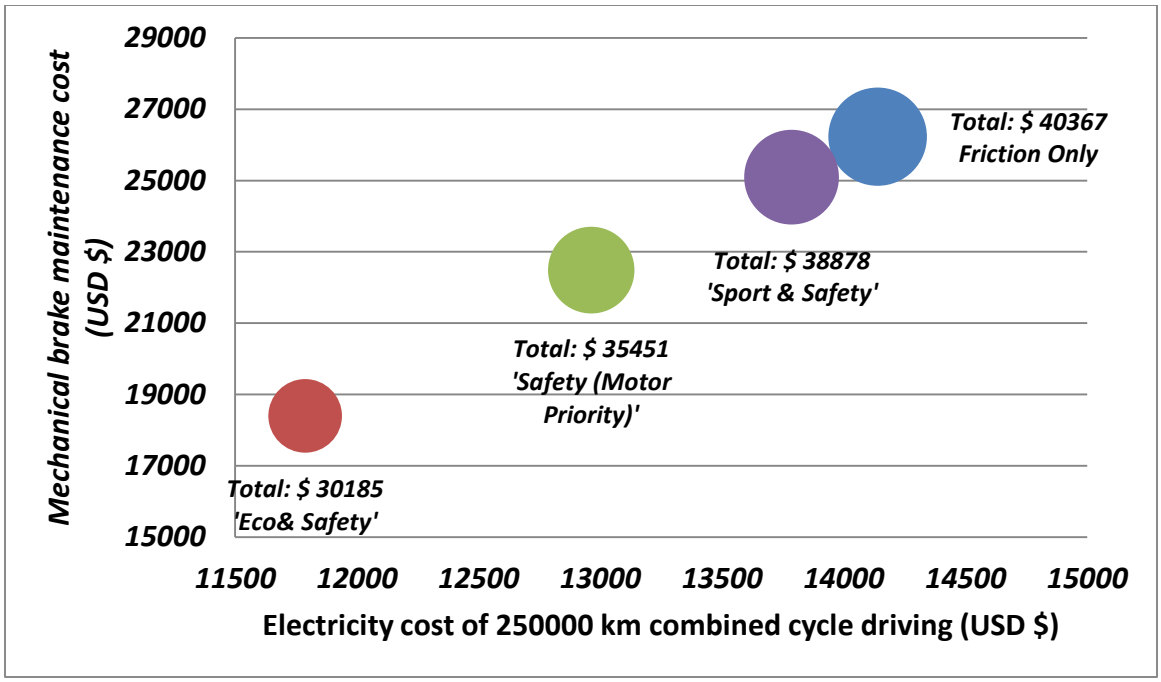

Figure 23: Maintenance and electricity cost of regenerative brake equipped BEV in 'Eco' strategy

9. Summary

This paper commenced by reporting the significant kinetic energy recovery potential in daily driving. The structure and advantage of front driven EV, especially for braking energy recovery, were discussed in detail. The factors which restrict blended braking were analyzed to determine the available regenerative braking from the motor, the ratio of motor and friction braking and the ratio of front and rear braking. Then, three blended braking strategies, 'Eco', 'Sport' and 'Safety (Motor Priority)' with their characteristics, were proposed, the latter optimizing braking energy recovery and improving braking performance simultaneously. A 'motor fault insurance' strategy was developed to avoid any unexpected and fatal error in motor braking system.

Several braking testing maneuvers were used in this paper to test the possible safety issues, which may be caused by redistributing the braking force between the front/rear axles in a mechanical/regenerative braking system. The feasible solutions are analyzed and included in the specially designed algorithms. In a straight line braking test, the details of the braking force distribution between the front and rear wheels from the motor and hydraulic system are given in figures. Split Mu testing examined the influence on a blended braking strategy from load transfer, cornering and the road condition changing during emergency braking. A cooperation algorithm of RBS, EBD and ABS is proposed to provide safe, efficient blended braking. The possible braking torque interruption risk introduced by gear shifting is avoided by this specially designed strategy. The share of front/rear friction braking and motor regenerative braking in strategies for typical driving cycles were presented in charts. Consequently, the braking energy recovery rates for different driving cycles were calculated.

The performance of the ‘Eco’ blended braking strategy has been experimentally verified in driving cycles by an integrated powertrain testing bench in the Lab. Thanks to the powerful motor and relatively small required braking force, most of the braking events were covered by motor regenerative braking alone in both city and highway cycles. In other words, the motor, especially for BEV, has sufficient ability to meet the braking requirement in the daily use. Specifically, 23.3% and 14.1% energy recovery rates, for NEDC and HWFET respectively, were achieved by the powertrain with regenerative braking in ‘Eco’ mode in experimental testing. These figures were approximately 10% below the calculated values, representing good agreement between the simulation and the measurements.

Initial manufacture and daily-use cost savings by RBS were analyzed and compared to evaluate the three strategies. The outcomes show that vehicle equipped with RBS can achieve a longer driving range per charge, a lower ‘fuel’ cost and a lower battery pack price with same target driving range, and lower maintenance cost. In term of vehicle lifetime, savings of approximately US$10k in ‘Eco’, US$4-5k in ‘Safety (Motor Priority)’ and US$1-2k in ‘Sport’ are expected respectively, considering that friction braking is always required in all strategies for emergency braking.

In summary, the three blended braking strategies not only improve braking performance, enabling adaptive braking force control, shorter stopping distance when the load is changing, and seamless transfer within RBS, EBD and ABS, but they also save customer’s money.

References

[1] Hartley J, Day A, Campean I, McLellan RG, Richmond J. Braking System for a Full Electric Vehicle with Regenerative Braking 2010. doi:10.4271/2010-01-1680.

[2] Kubaisi R, Herold K, Gauterin F, Giessler M. Regenerative Braking Systems for Electric Driven Vehicles: Potential Analysis and Concept of an Adaptive System 2013. doi:10.4271/2013-01-2065.

[3] Zhang J, Lv C, Qiu M, Li Y, Sun D. Braking energy regeneration control of a fuel cell hybrid electric bus. Energy Convers Manag 2013;76:1117–24. doi:10.1016/j.enconman.2013.09.003.

[4] Liu T, Zheng J, Su Y, Zhao J. A study on control strategy of regenerative braking in the hydraulic hybrid vehicle based on ECE regulations. Math Probl Eng 2013;2013. doi:10.1155/2013/208753.

[5] Nian X, Peng F, Zhang H. Regenerative Braking System of Electric Vehicle Driven by Brushless DC Motor. IEEE Trans Ind Electron 2014;61:5798–808. doi:10.1109/TIE.2014.2300059.

[6] Han J, Park Y. Cooperative regenerative braking control for front-wheel-drive hybrid electric vehicle based on adaptive regenerative brake torque optimization using under-steer index. Int J Automot Technol 2014;15:989–1000. doi:10.1007/s12239-014-0104-9.

[7] Zhou Z, Mi C, Zhang G. Integrated control of electromechanical braking and regenerative braking in plug-in hybrid electric vehicles Zhiguang Zhou Guixiang Zhang. Int J Veh Des 2012;58:223–39.

[8] Gao Y, Chen L, Ehsani M. Investigation of the Effectiveness of Regenerative Braking for EV and HEV 1999. doi:10.4271/1999-01-2910.

[9] Zhang J, Lv C, Yue X, Qiu M, Gou J, He C. Development of the Electrically-Controlled Regenerative Braking System for Electrified Passenger Vehicle 2013. doi:10.4271/2013-01-1463.

[10] Kim J, Yim E, Jeon C, Jung C, Han B. EFFECT OF REGENERATIVE BRAKING ENERGY ON BATTERY CURRENT BALANCE IN A PARALLEL HYBRID GASOLINE-ELECTRIC VEHICLE UNDER FTP-75 DRIVING MODE. Int J Automot Technol 2016;17:865–72. doi:DOI 10.1007/s12239−016−0084−z.

[11] Lv C, Zhang J, Li Y, Yuan Y. Novel control algorithm of braking energy regeneration system for an electric vehicle during safety-critical driving maneuvers. Energy Convers Manag 2015;106:520–9. doi:10.1016/j.enconman.2015.09.062.

[12] Li L, Zhang Y, Yang C, Yan B, Marina Martinez C. Model predictive control-based efficient energy recovery control strategy for regenerative braking system of hybrid electric bus. Energy Convers Manag 2016;111:299–314. doi:10.1016/j.enconman.2015.12.077.

[13] Di Nicola F, Sorniotti A, Holdstock T, Viotto F, Bertolotto S. Optimization of a multiple-

783 mpeed transmission for downsizing the motor of a fully electric vehicle. SAE Int J Alt
784 Power 2012;1:134–43. doi:10.4271/2012-01-0630.

785 [14] Bottiglione F, De Pinto S, Mantriota G, Sorniotti A. Energy consumption of a battery
786 electric vehicle with infinitely variable transmission. Energies 2014;7:8317–37.
787 doi:10.3390/en7128317.

788 [15] Jun-Qiang X, Guang-Ming X, Yan Z. Application of automatic manual transmission
789 technology in pure electric bus. 2008 IEEE Veh Power Propuls Conf VPPC 2008 2008:5–8.
790 doi:10.1109/VPPC.2008.4677583.

791 [16] Walker PD, Abdul Rahman S, Zhu B, Zhang N. Modelling, simulations, and optimisation of
792 electric vehicles for analysis of transmission ratio selection. Adv Mech Eng 2013;2013.
793 doi:10.1155/2013/340435.

794 [17] Ruan J, Walker P. An Optimal Regenerative Braking Energy Recovery System for Two-
795 Speed Dual Clutch Transmission-Based Electric Vehicles 2014. doi:10.4271/2014-01-1740.

796 [18] Infantini MB, Britto JFFH, Perondi E. Model of an ABS pneumatic regenerative braking
797 system 2005. doi:10.4271/2005-01-4033.

798 [19] Conlon B, Kidston K. Electric vehicle with regenerative and anti-lock braking, 1997.

799 [20] Lv C, Zhang J, Li Y, Yuan Y. Mechanism analysis and evaluation methodology of
800 regenerative braking contribution to energy efficiency improvement of electrified
801 vehicles. Energy Convers Manag 2015;92:469–82. doi:10.1016/j.enconman.2014.12.092.

802 [21] Ruan J, Walker P, Zhang N, Xu G. The safety and dynamic performance of blended brake
803 system on a two-Speed DCT based battery electric vehicle. SAE Int J Passeng Cars-
804 Mechanical Syst 2016;9:143–53. doi:10.4271/2016-01-0468.

805 [22] Ruan J, Walker P, Zhang N. A comparative study energy consumption and costs of battery
806 electric vehicle transmissions. Appl Energy 2016;165:119–34.
807 doi:10.1016/j.apenergy.2015.12.081.

808 [23] Genta G, Morello L, editors. The Automotive Chassis: Vol. 2: System Design, Dordrecht:
809 Springer Netherlands; 2009, p. 231–45. doi:10.1007/978-1-4020-8675-5_8.

810 [24] REGULATION (EC) No 661/2009 OF THE EUROPEAN PARLIAMENT AND OF THE COUNCIL of
811 13 July 2009. Off J Eur Union 2009:1–24.

812 [25] Regulation No. 13-H Uniform provisions concerning the approval of passenger cars with
813 regard to braking. UNITED 2014:97.

814 [26] Regulation No. 13 Uniform provisions concerning the approval of vehicles of categories
815 M, N and O with regard to brkaing 2002:1–194.

816 [27] Oleksowicz SA, Burnham KJ, Southgate A, McCoy C, Waite G, Hardwick G, et al.
817 Regenerative braking strategies, vehicle safety and stability control systems: critical use-
818 case proposals. Veh Syst Dyn 2013;51:684–99. doi:10.1080/00423114.2013.767462.

819 [28] National Highway Traffic Safety Administration Laboratory Test Procedure for 2005.

[29] Emission Test Cycles: ECE 15 + EUDC / NEDC n.d. https://www.dieselnet.com/standards/cycles/ece_eudc.php (accessed March 31, 2016).

[30] EPA U. EPA Urban Dynamometer Driving Schedule (UDDS) | Emission Standards Reference Guide | US EPA n.d. https://www3.epa.gov/otaq/standards/light-duty/udds.htm (accessed March 31, 2016).

[31] EmissionTest Cycles: EPA Highway Fuel Economy Test Cycle n.d. https://www.dieselnet.com/standards/cycles/hwfet.php (accessed March 31, 2016).

[32] EPA U. LA92 “Unified” Dynamometer Driving Schedule | Emission Standards Reference Guide | US EPA n.d. https://www3.epa.gov/otaq/standards/light-duty/la92.htm (accessed March 31, 2016).

[33] Emission Test Cycles: Japanese 10-15 Mode n.d. https://www.dieselnet.com/standards/cycles/jp_10-15mode.php (accessed March 31, 2016).

[34] Hsu Y-HJ. Estimation and control of lateral tire forces using steering torque. STANFORD UNIVERSITY, 2009.

[35] Chu L, Yao L, Chen J, Chao L, Guo J, Zhang Y, et al. Integrative braking control system for electric vehicles. 2011 IEEE Veh Power Propuls Conf VPPC 2011 2011. doi:10.1109/VPPC.2011.6042995.

[36] Mehrdad Ehsani, Yimin Gao, Ali E. Modern electric, hybrid electric and fuel cell vehicles: fundamentals, theory, and design. 2nd ed, CRC Press, 2009. ISBN: 9781420053982

[37] Huinink H, Volk H, Becke M. Bremsenhandbuch: Grundlagen, Komponenten, Systeme, Fahrdynamik. In: Breuer B, Bill HK, editors., Wiesbaden: Vieweg+Teubner Verlag; 2012, p. 65–84. doi:10.1007/978-3-8348-2225-3_5.

[38] National Highway Traffic Safety Adminstration UD. Evaluation of Enhanced Brake Lights Using Surrogate Safety Metrics. 2010.

[39] Volvo Car Corporation. The All New VOLVO XC70. 2013.

[40] National Highway Traffic Safety Adminstration UD. Automatic Emergency Braking System (AEB) Research Report. 2014.

[41] Yilmaz EH, Warren WH. Visual control of braking: A test of the ṫ hypothesis. J Exp Psychol Hum Percept Perform 1995;21:996–1014.

[42] Hart PM. Development of the Australian Brake Balance code of practice. Hartwood Consult Pty Ltd 2010:1–19.

[43] Energy V. 12.8 Volt Lithium-Iron-Phosphate Batteries n.d. https://www.victronenergy.com/upload/documents/Datasheet-12,8-Volt-lithium-iron-phosphate-batteries-EN.pdf.

[44] Zhang J, Li Y, Lv C, Yuan Y. New regenerative braking control strategy for rear-driven electrified minivans. Energy Convers Manag 2014;82:135–45.

857 doi:10.1016/j.enconman.2014.03.015.
858 [45] Berry IM. The effects of driving style and vehicle performance on the real world fuel
859 consumption of US light duty vehicles. Massachusetts Institute of Technology, 2010.
860 [46] Björnsson L-H, Karlsson S. The potential for brake energy regeneration under Swedish
861 conditions. Appl Energy 2016;168:75–84. doi:10.1016/j.apenergy.2016.01.051.
862 [47] Lu S. Vehicle survivability and travel mileage Schedules. Natl Tech Inf Serv 2006:40.
863 [48] U.S. Environmental Protection Agency. Greenhouse gas emissions from a typical
864 passenger vehicle 2014:1–5.
865 [49] Transportation, U.S. Department BOTS. National Transportation Statistics 2015:1–470.
866 [50] Saxena S, MacDonald J, Moura S. Charging ahead on the transition to electric vehicles
867 with standard 120 V wall outlets. Appl Energy 2014;157:720–8.
868 doi:10.1016/j.apenergy.2015.05.005.
869 [51] Bi Z, Song L, De Kleine R, Mi CC, Keoleian GA. Plug-in vs. wireless charging: life cycle
870 energy and greenhouse gas emissions for an electric bus system. Appl Energy
871 2015;146:11–9. doi:10.1016/j.apenergy.2015.02.031.
872 [52] Laboratory ORN. Plug-in hybrid electric vehicle value proposition study. US Dep ENERGY
873 2010:218.
874 [53] Kinghorn R, Kua D. Forecast uptake and economic evaluation of electric vehicles in
875 victoria. Melbourne: 2011.
876 [54] Cluzel C, Douglas C. Cost and performance of EV batteries: Final report for The
877 Committee on Climate Change. 2012.
878 [55] Newbery D, Strbac G. What is the target battery cost at which Battery Electric Vehicles
879 are socially cost competitive ? , Energy Policy Research Group University of Cambridge,
880 2014.
881 [56] Omar N, Monem MA, Firouz Y, Salminen J, Smekens J, Hegazy O, et al. Lithium iron
882 phosphate based battery – Assessment of the aging parameters and development of
883 cycle life model. Appl Energy 2014;113:1575–85.
884 doi:http://dx.doi.org/10.1016/j.apenergy.2013.09.003.
885 [57] Swierczynski M, Stroe D-I, Stan A-I, Teodorescu R, Kaer SK. Lifetime Estimation of the
886 Nanophosphate LiFePO4/C Battery Chemistry Used in Fully Electric Vehicles. IEEE Trans
887 Ind Appl 2015;51:3453–61. doi:10.1109/TIA.2015.2405500.
888 [58] Omar N, Monem MA, Firouz Y, Salminen J, Smekens J, Hegazy O, et al. Lithium iron
889 phosphate based battery – Assessment of the aging parameters and development of
890 cycle life model. Appl Energy 2014;113:1575–85. doi:10.1016/j.apenergy.2013.09.003.
891 [59] Deshpande R, Verbrugge M, Cheng Y-T, Wang J, Liu P. Battery Cycle Life Prediction with
892 Coupled Chemical Degradation and Fatigue Mechanics. J Electrochem Soc
893 2012;159:A1730–8. doi:10.1149/2.049210jes.

[60] Hu C, Jain G, Tamirisa P, Gorka T. Method for estimating capacity and predicting remaining useful life of lithium-ion battery. Appl Energy 2014;126:182–9. doi:10.1016/j.apenergy.2014.03.086.

[61] Saft. Lithium-ion battery life. 2014.

[62] Onat NC, Kucukvar M, Tatari O. Conventional, hybrid, plug-in hybrid or electric vehicles? State-based comparative carbon and energy footprint analysis in the United States. Appl Energy 2015;150:36–49. doi:10.1016/j.apenergy.2015.04.001.

[63] Grochowicz J, Grabiec T. Potential for commonization of brake testing for globally marketed vehicles 2009. doi:10.4271/2009-01-3031.

[64] Brake pads replacement cost guide n.d. http://www.brakepadscostguide.com/ (accessed February 24, 2016).

[65] Brake pads cost guide: average brake pad replacement cost n.d. https://autoservicecosts.com/brake-pad-replacement-cost/ (accessed February 24, 2016).

911 ## Appendix

912 The summaries of vehicle specifications in powertrain testing rig are presented in Table.1A:

913 Table 1A: Vehicle Specifications

Parameter	Description	Value	Units
m	Vehicle mass (incl. battery)	1500	kg
δm	Equivalent mass (Incl. Rotation part)	1.1m	kg
r	Tire radius	0.3125	m
i_g	Gear ratio	8.45/5.36	-
C_R	Coefficient of rolling resistance	0.016	-
h_g	Height of centre of mass	0.5	m
L	Length of wheelbase	2.675	m
L_a	Length of front axle centre of mass	1.2	m
L_b	Length of rear axle centre of mass	1.476	m
ϕ	Road incline	-	%
C_D	Aerodynamic Drag coefficient	0.28	-
A	Vehicle frontal area	2.2	m^2
u	Vehicle speed	-	m/s
T_{peak}/T_{rated}	Motor peak/rated output torque	300/150	Nm
P_{peak}/P_{rated}	Motor peak/rated output power	125/45	Kw
n_{peak}	Max speed of peak torque	2500	rpm
n_{max}	Max motor speed	8000	rpm
V_{bat}	Battery voltage	380	V

C_{bat}	Battery capacity	40	Ah
E_{bat}	Battery energy content	27.4	kWh

914

915

Contact Information

Jiageng Ruan

Mobil: +61 0450580627

E-MAIL: JIAGENG.RUAN@STUDENT.UTS.EDU.AU

Mail Address: Unit T02, 4-12 Garfield St, Five Dock 2046, AUSTRALIA

Acknowledgments

The authors would like to thank the Australian Research Council for financial support under grant DP150102751 for their financial support. Jiageng Ruan would also like to thank the Chinese Scholarship Council and University of Technology Sydney for financial support for his research and grateful to Prof. Nong Zhang, Prof Perter Waterson and Dr. Paul Walker for their valuable advice.

928 **Definitions/Abbreviations**

BEV	Battery Electric Vehicle
DCT	Dual Clutch Transmission
AT	Automatic Transmission
AMT	Automated Manual Transmission
CVT	Continuously Variable Transmission
VCU	Vehicle Control Unit
ABS	Anti-Lock Brake System
EBD	Electro Control Brake Distribution
RBS	Regenerative Brake System
SOC	State of Charge
MPC	Mileage per cycle
CPK	Consumed energy per km
RPK	Recovered braking energy per km

929